Copyright Warning & Restrictions

The copyright law of the United States (Title 17, United States Code) governs the making of photocopies or other reproductions of copyrighted material.

Under certain conditions specified in the law, libraries and archives are authorized to furnish a photocopy or other reproduction. One of these specified conditions is that the photocopy or reproduction is not to be "used for any purpose other than private study, scholarship, or research." If a, user makes a request for, or later uses, a photocopy or reproduction for purposes in excess of "fair use" that user may be liable for copyright infringement,

This institution reserves the right to refuse to accept a copying order if, in its judgment, fulfillment of the order would involve violation of copyright law.

Please Note: The author retains the copyright while the New Jersey Institute of Technology reserves the right to distribute this thesis or dissertation

Printing note: If you do not wish to print this page, then select "Pages from: first page # to: last page #" on the print dialog screen

ABSTRACT

INTERFERENCE CANCELLATION BY TIME ADJUSTABLE SAMPLING

by
Josko Zec

The problem of improving the frequency response of linear arrays is addressed in this thesis. The improvement is measured in the level of rejection of the undesired sources. A new, simple, and practical method is suggested. It is based on adjusting the sampling time in selected channels. Interference cancellation for finite bandwidth signals is accomplished only at, or close to, the carrier frequency. Wideband cancellation requires additional hardware and computational complexity. Conventional way of the wideband interference cancellation utilizes tapped delay line adaptive filters in each channel.

The Time Adjustable Sampling (TAS) method achieves a part of the tapped delay line effect by adjusting the sampling time in some selected array channels. Signal beamforming is combined with TAS. The beamforming is done using complex weights. The combination of the complex weights and TAS provides improvement over the usage of the complex weights only. Hardware and computational requirements in implementing the TAS method are significantly lower than for the tapped delay line structure of the same dimension.

Different configurations are investigated. The comparison with a conventional method is given. It was found that TAS significantly improves wideband linear prediction. A computer simulation confirmed results obtained by the model analysis.

INTERFERENCE CANCELLATION BY TIME ADJUSTABLE SAMPLING

by
Josko Zec

A Thesis
Submitted to the Faculty of
New Jersey Institute of Technology
in Partial Fulfillment of the Requirements for the Degree of
Master of Science in Electrical Engineering

Department of Electrical and Computer Engineering

May 1994

APPROVAL PAGE

INTERFERENCE CANCELLATION BY TIME ADJUSTABLE SAMPLING

Josko Zec

Dr. Alexander Haimovich, Thesis Advisor Associate Professor of Electrical and Computer Engineering, NJIT	Date
Dr. Wan-Ling Chen, Committee Member Adjunct Professor of Electrical and Computer Engineering, NJIT	Date
Dr. Joseph Frank, Committee Member Associate Professor of Electrical and Computer Engineering, NJIT	Date

BIOGRAPHICAL SKETCH

Author: Josko Zec

Degree: Master of Science in Electrical Engineering

Date: May 1994

Undergraduate and Graduate Education:

- Master of Science in Electrical Engineering,
  New Jersey Institute of Technology, Newark, NJ, 1994

- Bachelor of Science in Electrical Engineering,
  University of Zagreb, Zagreb, Croatia, 1992

Major: Electrical Engineering

ACKNOWLEDGMENT

I would like to express deep gratitude to my supervisor, Professor Alexander Haimovich for his patience, support and help throughout this research.

I would like to thank Dr. Joseph Frank and Dr. Wan-Ling Chen for serving as members of the committee.

I appreciate all suggestions from the Communications Laboratory members, including: Aparna Vadhri, Lisa Fitton, Andrew Bateman, Michael Meyer, and Chris Peckham.

TABLE OF CONTENTS

Chapter Page

LIST OF FIGURES

Figure Page

CHAPTER 1

INTRODUCTION

One of the main tasks of the radar system is spatial filtering; meaning the reception of signals from a desired direction while discriminating against signals arriving from other directions. This task can be fulfilled by narrow antenna beams as well as by appropriate signal processing of the outputs of an antenna array. signal processing offers more flexibility and enables adaptive operation in various interference environments. Adaptive antennas adjust their response according to the environment they are operating in. The emphasis is shifted from the beamwidth and the sidelobe level to other parameters. These parameters could be Signal-to-noise-plus-interference ratio (SNIR), the error between the desired and the received signal, or the time needed to adapt to changes in the interference environment, to name a few. An extensive introduction to the adaptive arrays is given in [7]. The author uses term "smart arrays" since an adaptive array utilizes far more information than a non-adaptive array which has a fixed response. The information is extracted by suitable processing of the received signal. Adaptive arrays in radar applications are designed to maximize the SNIR.

The tendency to operate modern radars in a wide frequency range is motivated by several facts. Operation in a broader frequency interval decreases susceptibility to countermeasures (intentional jamming) and increases the ability for the adjustment to the changes in the environmental conditions. However, the advantages of the wideband capability are accompanied with the requirement to suppress the unwanted signals at all frequencies in the receiver passband. As the bandwidth becomes wider, it is more difficult to cancel the unwanted signals across the entire band.

Research summarized in this thesis addresses a possible method for the wideband adaptive interference cancellation. The method is based on time adjustable

sampling (TAS). The essence of the TAS method is control of the timing of sampling of the received signals. The idea is that the proper adjustment of the sampling would compensate for the propagation delay across the array. It is assumed that the signals are received by a linear, uniformly spaced antenna array. It is expected that implementing time delays in one or more of the array elements would lead to a better interference cancellation than using the beamforming only. The complex beamforming is implemented using phase shifts which are easy to implement by complex weighting of baseband signals. The improvement is intuitively plausible since the time delays would introduce frequency dependence and thus provide compensation in the frequency band of interest.

The TAS method is designed in conjuction with Airborne Early Warning (AEW) Radar Testbed which is developed for the US Navy. The AEW Radar Testbed program is intended to provide the Navy with a platform that enables testing of new radar concepts. The more detailed introduction to the AEW Radar Testbed is given in [20]. This thesis aims to investigate the TAS method and show its applicability to the problem of the wideband interference cancellation. The method is to be tested in the AEW Radar Testbed. Few important antenna limitations and effects are not taken into account in the thesis. Some of these are polarization, multi-path effects, antenna dispersion, and channel mismatches. These effects are unavoidable in practice and can affect results significantly. Our analysis assumes identical response of all sensors. Since this perfect matching of the channel transfer functions is unachievable, results will present the ideal case.

Theory for the narrowband interference cancellation is addressed in the books ([4], [12], and [15]). The goal of the processing is to find the optimal weight vector which, when applied to the input signals, would provide lowest interference at the output. Input signals appear at a single frequency. Well-developed solutions exist for this problem. Correlation matrices and steering vectors appearing in these solutions

are simple and enable analytical solutions for the optimal weight vector. The optimal weight vector is calculated using some known feature of the desired signal or the interference. This known feature can be extracted from the received signal. If the direction of the desired signal is known, the goal is to maximize the response from that direction relative to the response from the direction of the interference. Efficient algorithms are derived to compute weight coefficients. Current research in the field of the narrowband interference cancellation is concerned with the improvement of the existing algorithms. This improvement is in terms of computational complexity and speed of convergence. In this thesis, only the steady-state solutions will be used, without considering the particular algorithms for getting these solutions.

Since the TAS method is essentially a wideband method, more attention is given to the problem of the wideband interference cancellation. Previous work in the wideband interference cancellation is concentrated around the tapped delay line structure. A detailed discussion about the tapped delay line method is given in [4] and [15]. Frequency dependence is achieved using delay lines. These delay lines produce phase shifts that change with frequency. Combining the proper tap spacing and the complex weight coefficients, frequency compensation can be accomplished. Each sensor is followed by a number of delay lines. Delay line outputs are adaptively weighted and summed to produce low interference level at the output of the processor. The structure for one channel is shown on Figure 1.1. The Time delay line structure is in fact a transversal FIR filter ([11]). Symbol Z^{-1} represents a time delay element and $w_o, w_1 .... w_{L-1}$ are adjustable complex weights. The final processor output is obtained by summing the outputs from every sensor such as shown in Figure 1.1. The number of complex coefficients to be computed is NL where N is the number of sensors in the array and L is the number of taps following each sensor. This approach entails increased hardware complexity and results in a higher dimensionality problem than narrowband beamforming. For a large number of elements and delay lines, the

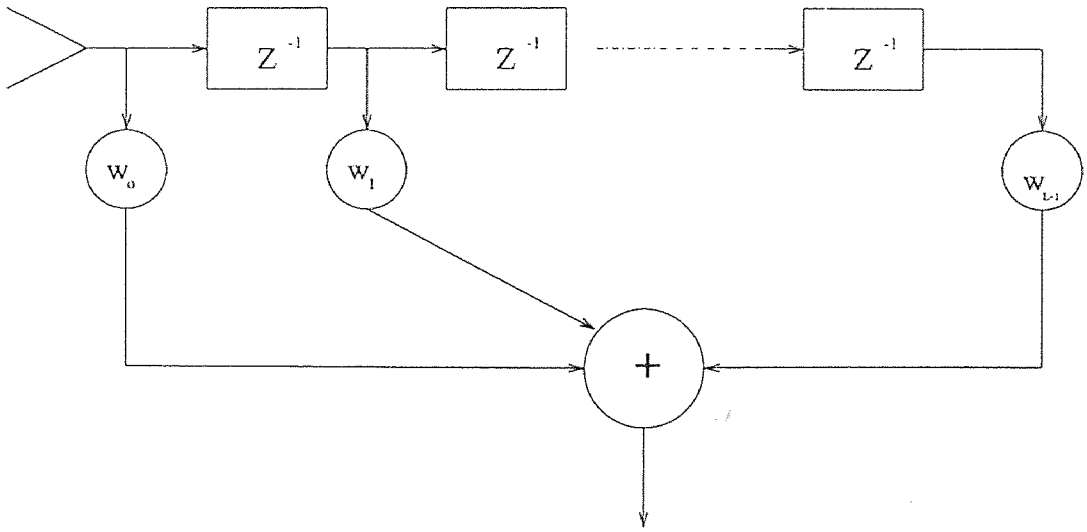

Figure 1.1 The tapped delay line structure.

problem becomes hardware and computationally costly. The TAS method achieves some of the effect of the tapped delay lines by only adjusting the sampling time in one or more channels. Our analysis will focus on the case of implementing TAS in one of the array elements. This case is easy to calculate and realize. It will be shown that the improvement over implementation with the phase shifts only, is achieved even for this simple case.

Several aspects of the tapped delay line method have been investigated in the literature. In [14] antenna dispersion and channel mismatches have been evaluated. It is shown that the wideband performance is determined by the spread of eigenvalues of the input correlation matrix. Larger eigenvalue spread leads to a lower cancellation achievable.

In [6] an algorithm for the linearly constrained adaptive array has been described. The constraint has been applied to the look-direction response which has been fixed. Therefore, the minimization of the total output power corresponds to the minimization of the undesired non-look direction power. The algorithm is proven to be able to correct the computational errors. The important requirement

is that the non-look direction noise is not correlated with the look-direction signal. Otherwise, a part of the desired signal would be cancelled. This can happen when the desired signal is received from more than a single path. On the other hand, it is desirable that the interference signals at the tap outputs are correlated.

A possible way to overcome the interference / desired signal correlation is suggested in [17]. The level of the cancellation of the desired signal depends on the correlation coefficient. The broadband frequency focusing was used and it was shown that the desired signal is not cancelled despite being correlated with the interference.

Reference [5] deals with the influence of the different parameters on the tapped delay line performance. The increase in the number of taps per sensor improves the frequency response. The choice of the optimal tap spacing is also discussed. It is found that using uniform tap spacings, it is possible to cancel the interference for only some angles of arrival of the interference. Eigenvalue analysis is also presented. Planar arrays processed with the tapped delay lines have shown strong dependence on the array configuration.

All works mentioned in this short literature survey assist as an introduction to the problem of the wideband interference cancellation. Analytical results are unavailable for the cases of more than two taps per sensor. The complexity associated with the implementation of the tapped delay lines motivates us to seek simpler solutions. The TAS is an attempt to use a simpler solution for the problem of the wideband interference cancellation.

The thesis is organized as follows: This introductory chapter defines the problem. It also mentions the existing solutions found in the literature. In Chapter 2 the Minimum Variance Beamformer (MVB) for the narrowband case is presented. Procedures for evaluating the array performance are outlined. Closed-form expressions are derived and the frequency response is calculated. A block-diagram implementation is proposed. Chapter 3 introduces the TAS method .

The optimal subarray weight vector is calculated. The cancellation performance is evaluated and compared with the MVB. The optimal time delay is found. A block-diagram implementation is proposed. The deterministic case is also addressed as well as the partitioning of the N-element array into modules. Processing within the modules is studied as well as combining the modules to yield the system output. The best results are obtained when complex weights and time delay are employed both at the element and at the module level. Chapter 4 deals with the wideband interfering signals. These signals have baseband frequency components that can not be neglected relative to the carrier frequency. Flat spectrum is assumed and correlation matrix is calculated for the entire bandwidth. Using this correlation matrix, the optimal weight vector is found and the cancellation is examined for different cases of bandwidths and interference-to-noise ratios. In Chapter 5 three additional cancellation structures are introduced. Each of these structures is analysed using the same mathematical model. Numerical results were calculated for some concrete realizations. It was shown that the structure denoted as TAS4 provides the lowest gain in the interference direction. The structure denoted TAS2 was shown to be equivalent to the MVB. In Chapter 6 computer simulations are used to evaluate the performance. The simulation procedure is briefly outlined. Few results are shown illustrating the main tendencies. Simulation results showed a high level of consistency with the calculation results. Chapter 7 concludes the work with a brief overview of the most important conclusions that can be drawn from the results obtained throughout the research.

CHAPTER 2

MINIMUM VARIANCE BEAMFORMER

2.1 Introduction

Minimum Variance Beamformer (MVB) is a conventional way of the adaptive signal processing. It is based on solving the Wiener equations for the optimal weight vectors ([11]). Before addressing the MVB specifically, the array and the signal representation are described in this introduction and in the following section.

It is assumed that the signal is received with a (N+1)- element linear array. The uniform spacing d between the array elements is assumed. This spacing needs to meet the criterion that $d \leq \lambda/2$, where λ is the wavelength corresponding to the frequency which radar is tuned to (f_c). In this chapter only narrowband signals are considered. Therefore, everything is observed at f_c and $\lambda = c/f_c$, where c is the speed of light. The condition that $d \leq \lambda/2$ prevents the appearance of the grating lobes. In the further development, $d = \lambda/2$ has been selected.

The propagation time delay between the two array elements is given as $\tau = d\sin\Theta/c$, where Θ denotes the angle between the direction of arrival and the normal to the array. Because of the uniform spacing, the time delay between the two neighbouring elements will be constant across the array. If a signal arrives from the direction orthogonal to the array ($\Theta = 0$), there is no time delay and the signal arrives at every sensor with the same phase. It will be assumed throughout the thesis that the desired signal arrives from $\Theta = 0$ angle. This assumption can be taken when the direction of arrival is known. In this case, regardless of the actual angle, an adjustment can be made as if the signal arrives from the broadside. The adjustment is done using the proper phase shifts after each element. The angle of arrival of the interference will be assumed unknown.

2.2 Signal Representation

Since there is a time delay τ between the array elements, the received signals will differ from element to element. If sensor 1 is taken as the reference point, the signals at the sensors will be:

Sensor 1: $x_1(t) = p(t)e^{-j\omega_c t}$

Sensor 2: $x_2(t) = p(t-\tau)e^{-j\omega_c(t-\tau)}$

and so forth up to the

Sensor N+1: $x_{N+1}(t) = p(t-N\tau)e^{-j\omega_c(t-N\tau)}$,

where $p(t)$ represents the waveform in the time-domain. These signals can be transformed to the frequency domain:

Sensor 1: $X_1(\omega) = P(\omega - \omega_c)$

Sensor 2: $X_2(\omega) = P(\omega - \omega_c)e^{-j\omega\tau}$

and so forth up to the

Sensor N+1: $X_{N+1}(\omega) = P(\omega - \omega_c)e^{-j\omega N\tau}$,

where $P(\omega)$ denotes the frequency-domain counterpart of $p(t)$. This suggests a vector representation of the array input:

$$\underline{x}(\omega) = P(\omega - \omega_c)\underline{d}, \tag{2.1}$$

where $\underline{d}$ is the steering vector defined as:

$$\underline{d}^T(\omega) = [1 \quad e^{-j\omega\tau} \quad e^{-2j\omega\tau} \cdots e^{-j\omega N\tau}], \tag{2.2}$$

where the superscript T denotes the transpose operation. Steering vectors define the direction of arrival of the signal.

The received signal is modelled as consisting of the desired part ($\underline{x}_d$), discrete interference ($\underline{x}_i$) and random noise ($\underline{x}_n$):

$$\underline{x}(\omega) = \underline{x}_d(\omega) + \underline{x}_i(\omega) + \underline{x}_n(\omega). \tag{2.3}$$

The desired signal is assumed to arrive from 90^o ($\Theta_d = 0$) and is delay-free:

$$\underline{x}_d(\omega) = P_d(\omega - \omega_c)[1 \quad 1 \cdots 1]^T = P_d(\omega - \omega_c)\underline{d}_o, \tag{2.4}$$

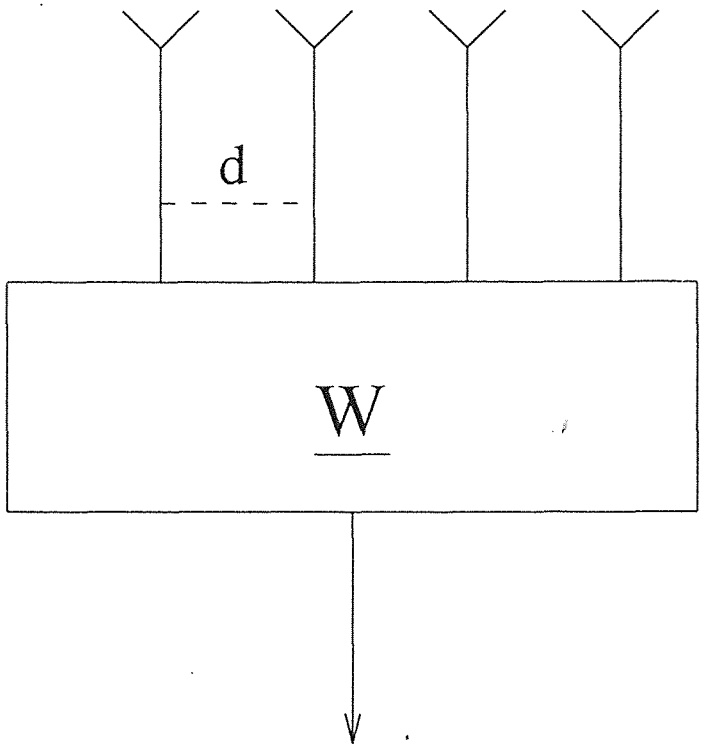

Figure 2.1 The MVB processor.

where $P_d(\omega - \omega_c)$ is the amplitude of the desired signal. The desired signal power can be neglected and $\underline{x}$ can be formed with only interference part $\underline{x}_i$ and noise part $\underline{x}_n$. It was shown in [15] that the power of the desired signal does not affect most of the results, so this assumption can be taken. This holds not only for the radar applications but for any antenna array. The interference signal is represented as:

$$\underline{x}_i(\omega) = P_i(\omega - \omega_c)[1 \quad e^{-j\omega\tau_i} \quad e^{-2j\omega\tau_i} \cdots e^{-Nj\omega\tau_i}]^T = P_i(\omega - \omega_c)\underline{d}_i(\omega), \qquad (2.5)$$

where $P_i(\omega - \omega_c)$ is the amplitude of the interference and $\tau_i = d\sin\Theta_i/c$ is the propagation time delay of the interference. Random noise vector $\underline{x}_n$ is taken as white in space; meaning the noise components at different sensors are uncorrelated. Since everything is observed only at a single frequency, the frequency spectrum of the noise is not of concern. Vector $\underline{x}$ is the input to the structure sketched in Figure 2.1.

The output of the MVB is obtained by weighting the inputs with the weight coefficients w_l, l=1,2 $\cdots$ N+1. Using the vector notation, the output can be expressed as the inner product:

$$Y(\omega) = \underline{w}^H \underline{x}(\omega), \tag{2.6}$$

where H denotes the Hermitian operator. In this chapter, the main concern is the narrowband case. It means that the optimal weight vector ($\underline{w}_o$) will be calculated at the carrier frequency. Using $\underline{w}_o$, frequency response will be found in a narrow band around the carrier frequency.

2.3 The Optimal Weight Vector

The objective can be stated: Minimize the total residual power subject to the constraint that the gain in the direction of the desired signal is unity. The constraint precludes the trivial solution $\underline{w}_o = \underline{0}$, where $\underline{w}_o$ denotes the optimal weight vector and $\underline{0}$ is the null-vector. The residual power is given by:

$$\begin{aligned} p_{res} &= E(|Y|^2) = E(YY^*) = E(\underline{w}^H \underline{x}(\underline{w}^H \underline{x})^H) \\ &= \underline{w}^H E(\underline{x}\,\underline{x}^H)\underline{w} \\ &= \underline{w}^H R \underline{w}, \end{aligned} \tag{2.7}$$

where R is the correlation matrix of the input vector:

$$R = E(\underline{x}\ \underline{x}^H). \tag{2.8}$$

Symbol * denotes the complex conjugate. Frequency dependence is ommited because everything is observed at ω_c.

The response of the MVB in the direction of the desired signal is given by:

$$\underline{w}_o^H \underline{d}_o = 1. \tag{2.9}$$

The residual power under the constraint (2.9) is:

$$p_{res} = \underline{w}^H R \underline{w} - \lambda(\underline{w}^H \underline{d}_o - 1). \tag{2.10}$$

The second term in (2.10) does not increase the residual power if $\underline{w}$ is chosen to meet the linear constraint. The minimization of p_{res} can be obtained by taking derivative of p_{res} with respect to $\underline{w}^H$ and setting it to zero :

$$\frac{\delta p_{res}}{\delta \underline{w}^H} = R\underline{w}_o - \lambda \underline{d}_o = 0. \tag{2.11}$$

The optimal weight vector is :

$$\underline{w}_o = \lambda R^{-1}\underline{d}_o. \tag{2.12}$$

The Lagrange coefficient λ can be found from the constraint (2.9):

$$\begin{aligned} \underline{w}_o^H \underline{d}_o &= \lambda^*(R^{-1}\underline{d}_o)^H \underline{d}_o = 1 \\ \lambda &= \frac{1}{\underline{d}_o^H R^{-1}\underline{d}_o}. \end{aligned} \tag{2.13}$$

In expressing λ in (2.13), the fact that R is the Hermitian matrix ($R = R^H$, $R^{-1} = (R^{-1})^H$) has been used (otherwise R^{-1^H} would have been used). The denominator of (2.13) is a real number because it is a Hermitian form ([19]). To proceed with the calculation of the residual power, the correlation matrix is written in the form:

$$R = E(\underline{x}_i \ \underline{x}_i^H) + E(\underline{x}_n \ \underline{x}_n^H). \tag{2.14}$$

Desired signal has been neglected as discussed before. Since $\underline{x}_n$ is the Gaussian noise vector, $\underline{x}_i$ is uncorrelated with $\underline{x}_n$. The first term relates to the interference and can be expressed as $E[\underline{x}_i \underline{x}_i^H] = p_i \underline{d}_i \underline{d}_i^H$, where p_i is the power of the interference signal. The second term of (2.14) is the noise correlation matrix and is equal to $\sigma^2 I$, where I is the identity matrix and σ^2 is the variance of noise at each array element. Using (2.5) and (2.14), the correlation matrix can be expressed as:

$$R = p_i \underline{d}_i \ \underline{d}_i^H + \sigma^2 I. \tag{2.15}$$

Now the matrix inversion lemma ([12]) can be used to compute the inverse of R:

$$R^{-1} = \frac{1}{\sigma^2}(I - \frac{p_i \underline{d}_i \ \underline{d}_i^H}{\sigma^2 + p_i \underline{d}_i^H \underline{d}_i}). \tag{2.16}$$

Substituting (2.16) in (2.13) gives:

$$\lambda = \frac{\sigma^2}{\underline{d}_o^H \underline{d}_o - \frac{p_i \underline{d}_o^H \underline{d}_i \underline{d}_i^H \underline{d}_o}{\sigma^2 + p_i \underline{d}_i^H \underline{d}_i}}. \tag{2.17}$$

Substituting (2.4) and (2.5) in (2.17):

$$\lambda = \frac{\sigma^2}{(N+1) - \frac{p_i |s|^2}{\sigma^2 + p_i (N+1)}}, \tag{2.18}$$

where $s = \underline{d}_o^H \underline{d}_i$.

The final expression for the optimal weight vector is from (2.12):

$$\underline{w}_o = \frac{R^{-1} \underline{d}_o}{\underline{d}_o^H R^{-1} \underline{d}_o} \tag{2.19}$$

From (2.19), it is easily checked that the constraint (2.9) is indeed satisfied:

$$\underline{w}_o^H \underline{d}_o = (\frac{R^{-1} \underline{d}_o}{\underline{d}_o^H R^{-1} \underline{d}_o})^H \underline{d}_o = \frac{\underline{d}_o^H R^{-1} \underline{d}_o}{\underline{d}_o^H R^{-1} \underline{d}_o} = 1.$$

2.4 The Cancellation Property of the MVB

With the optimal weight vector found and given with (2.19), the interference cancellation property of the MVB can be shown. The residual power (p_{res}) after the MVB processing is given:

$$p_{res} = \underline{w}_o^H R \underline{w}_o = (\frac{R^{-1} \underline{d}_o}{\underline{d}_o^H R^{-1} \underline{d}_o})^H R \frac{R^{-1} \underline{d}_o}{\underline{d}_o^H R^{-1} \underline{d}_o}. \tag{2.20}$$

This simplifies to:

$$p_{res} = \frac{1}{\underline{d}_o^H R^{-1} \underline{d}_o}. \tag{2.21}$$

This is the same expression as for the Lagrange coefficient (2.13). Therefore, the residual power is given also with (2.18). The variable s in that expression is:

$$\begin{aligned} s &= \underline{d}_o^H \underline{d}_i = [1 \quad 1 \cdots 1][1 \quad e^{-j\omega_c \tau_i} \cdots e^{-Nj\omega_c \tau_i}]^T \\ &= \sum_{k=0}^{N} e^{-kj\omega_c \tau_i} \\ &= e^{-j\omega_c N/2} \frac{\sin(\omega_c (N+1)\tau_i/2)}{\sin(\omega_c \tau_i/2)} \\ |s|^2 &= \frac{\sin^2(\omega_c (N+1)\tau_i/2)}{\sin^2(\omega_c \tau_i/2)}. \end{aligned} \tag{2.22}$$

Substituting (2.22) into (2.18), the expression for the residual power becomes:

$$p_{res} = \frac{\sigma^2}{(N+1) - \frac{p_i}{\sigma^2 + p_i(N+1)} \frac{\sin^2(\omega_c(N+1)\tau_i/2)}{\sin^2(\omega_c\tau_i/2)}}. \tag{2.23}$$

For the simplicity, s will be kept instead of $\sin(Mx)/\sin(x)$ form. The power of the interference at the input will be assumed to be unity ($p_i = 1$), which leads to:

$$p_{res} = \frac{\sigma^2(\sigma^2 + N + 1)}{\sigma^2(N+1) + (N+1)^2 - |s|^2}. \tag{2.24}$$

Assuming that the power of the thermal noise is much below the interference power ($\sigma^2 \ll 1$):

$$p_{res} \approx \frac{\sigma^2}{(N+1) - \frac{1}{N+1}|s|^2}. \tag{2.25}$$

The critical point in (2.25) is when $\tau_i \to 0$ (this corresponds to $|s| = N+1$). Then the denominator goes to zero and it seems that p_{res} goes to infinity. This calls for the observation of (2.24), which is the exact expression rather than the approximation (2.25). If we let $\tau_i \to 0$ in (2.24) and $\sigma^2 \ll 1$, then p_{res} becomes unity and not infinity. That was expected since $\tau_i = 0$ means the arrival from the broadside direction. This direction is where the constraint has been imposed and the gain of unity has been fixed. Therefore, to obtain the cancellation, the interference must be sufficiently distant from the desired signal direction. In other words,

$$\frac{\sin(\omega_c(N+1)\tau_i/2)}{\sin(\omega_c\tau_i/2)} \ll (N+1) \tag{2.26}$$

must hold. When (2.26) holds, (2.24) can be approximated as (2.25). From (2.25) the cancellation is obvious because the denominator is greater than one. So for the case when τ_i is sufficiently greater then 0 (which corresponds to $|s| \ll N+1$), the conclusion is that $p_{res} \approx \sigma^2/(N+1)$.

2.5 Array Factor

Having found the optimal weight vector and having shown the cancellation property of the MVB, the next step is to investigate the frequency response of the array. The

frequency response (referred to as the array factor) will be calculated as the inner product of the optimal weight vector and the steering vector in the direction of the interference :

$$A_i(\omega) = |\underline{w}_o^H \underline{d}_i(\omega)|, \tag{2.27}$$

where $\underline{w}_o$ is given in (2.19) and $\underline{d}_i(\omega)$ is given in (2.5). The optimal weight vector has been calculated at the carrier frequency. On the other hand, this inner product will show the gain to the spectral components at the frequencies ω other than ω_c. However, this procedure is correct for the narrowband case. The criterion for the signal to be considered narrowband is that $Nd \ll c/B$, where Nd is the total length of the array and B is the bandwidth. The criterion is stated in ([12]) and will be derived in Chapter 4. We are using the narrowband approach in calculating the optimal weight vector because it enables the retrieval of the analytical results. If the narrowband criterion holds, the error in calculating the array factor using the narrowband optimal weight vector is negligible.

The steering vector to the desired signal $\underline{d}_o$ does not change with frequency because τ_o (desired signal propagation time delay) is assumed to be zero. So at every frequency:

$$\underline{d}_o^T(\omega) = [1 \quad 1 \cdots 1]. \tag{2.28}$$

The constraint (2.9) holds and is not affected by the change in frequency.

If the spectrum of the interference is flat, the array factor will be proportional to the output interference spectrum. For any arbitrary spectrum, the array factor is the gain that the MVB will provide in the direction of the interference. The goal of the processing is to make this gain as low as possible.

2.6 An Example and a Possible Implementation

In the calculation of the array factor (2.27), the following parameters are taken: Carrier frequency is chosen to be $f_c = 1$ GHz (L band), the array consists of 16

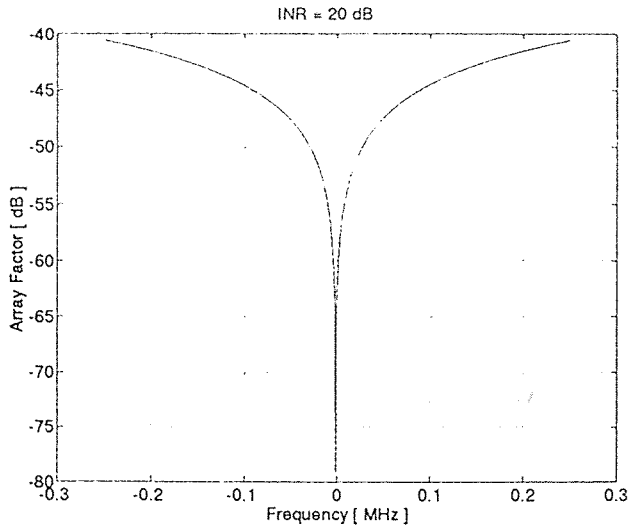

Figure 2.2 The array factor for the narrowband MVB.

elements, the angle of the interference is 60°, the power of the interference at the input is normalized as unity $p_i = 1$, and the variance of the noise is $\sigma^2 = 10^{-2}$. These are all parameters necessary for (2.27) which calculates the array factor for the interference. These parameters are chosen to represent a realistic scenario for the AEW Radar. Figure 2.2 shows the result of (2.27) for the parameters as defined. Array factor is calculated for the bandwidth of 500 KHz, which centered around 1 GHz justifies the narrowband assumption. For the given parameters, the total array length (Nd) is 2.25 m while the ratio c/B is 600 m. The criterion $Nd \ll c/B$ is satisfied. This example was given to illustrate the cancellation ability of the MVB in a realistic environment for the AEW Radar operation. From Figure 2.2, this ability is obvious. The extreme frequency components of the interference are attenuated as much as ≈ 40 dB.

A possible implementation of the MVB is sketched in Figure 2.3 in block-diagram form. It assumes prior knowledge of all parameters needed to calculate the weight vector. Taking the expected value $R = E(\underline{x}\,\underline{x}^H)$ in real time is not possible.

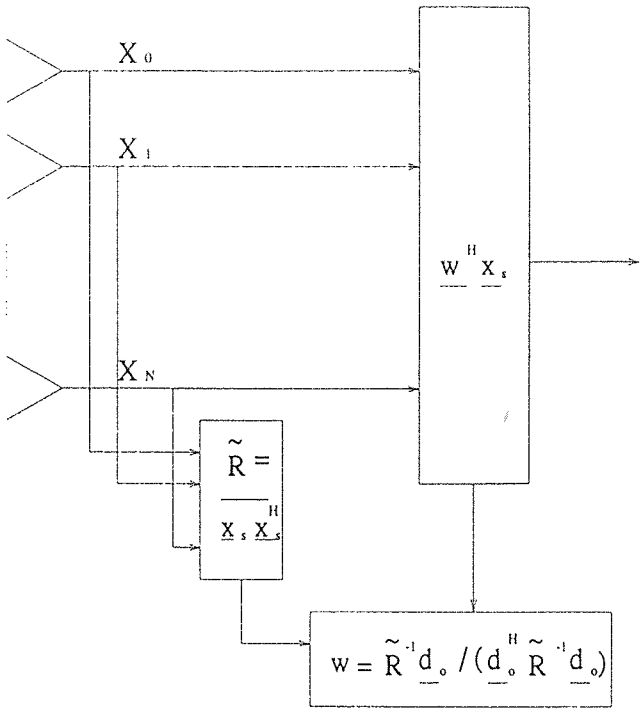

Figure 2.3 A possible implementation of the MVB.

$\tilde{R}$ is the estimation of the correlation matrix. Minimum variance estimation is:

$$\tilde{R} = \overline{\underline{x}\ \underline{x}^H} = \frac{1}{L}\sum_{l=1}^{L} \underline{x}_l\ \underline{x}_l^H. \tag{2.29}$$

A set of the input data vector is referred to as a "snapshot". The subscript l denotes the l-th snapshot of the input vector and L denotes the number of snapshots taken to estimate the correlation matrix.

CHAPTER 3

TIME ADJUSTABLE SAMPLING

3.1 Introduction

The Time Adjustable Sampling (TAS) method is based on the idea that implementing time delays in selected channels would lead to a better frequency response than using the phase shifts alone. This idea will be developed for the simplest case: the case of only one time adjustable channel. The representation of the signals will be consistent with the representation defined in Chapter 2. The TAS structure is sketched in Figure 3.1. The (N+1)-element array is divided in a N-element subarray and an auxiliary channel. The subarray output is formed as the inner product between the subarray weight vector $\underline{v}$ and the subarray input vector $\underline{x}_s$. Because the subarray contains N elements, these both vectors are N-by-1 as opposed to the (N+1)-by-1 vectors in the MVB. The subarray output is subtracted from the auxiliary channel output. The signal in the auxiliary channel is delayed to compensate for the propagation time delay across the array. The compensation time delay is denoted t_d. In order to simplify the expressions, the auxiliary channel is taken as a reference. It means there is no propagation delay in the auxiliary channel. The power of the desired signal is neglected and the angle of its arrival is assumed known. The idea is that the compensation time delay produces frequency dependent phase shifts. These phase shifts are expected to achieve some of the tapped delay line effect. This effect should manifest itself in a lower array factor, i.e., lower gain in the direction of the interference. In this chapter, narrowband TAS is considered.

Although the presented structure is essentially new, some ideas related to TAS can be found in the literature. In [13] the array has been divided in two separate subarrays. Desired signal was cancelled at the output of one subarray. The output has been formed by subtracting the outputs from these two subarrays. Since desired

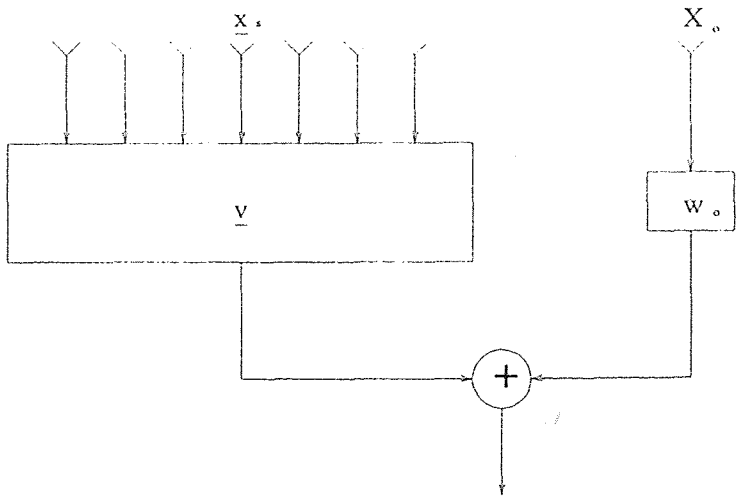

Figure 3.1 The TAS processor.

signal is cancelled in one subarray, the other subarray provided the desired signal. This idea is a part of the TAS structure.

3.2 The Subarray Optimal Weight Vector

The optimization problem for TAS can be stated: Minimize the residual power which is left after subtracting the subarray output from the auxiliary channel output. The residual power is given with:

$$p_{res} = |w_o X_o - \underline{v}^H \underline{x}_s|^2, \tag{3.1}$$

where X_o is the signal in the auxiliary channel, $\underline{v}$ is the subarray weight vector, and $\underline{x}_s$ is the subarray input vector. The weight coefficient w_o is realized with the time delay t_d and the fixed phase shift Φ:

$$w_o = e^{-j\omega t_d} e^{j\Phi}. \tag{3.2}$$

Everything is observed at ω_c (narrowband) where the phase shift is adjusted such that:

$$\Phi = \omega_c t_d. \tag{3.3}$$

Combining (3.2) and (3.3), w_o becomes one and (3.1) becomes:

$$\begin{aligned} p_{res} &= E[(X_o - \underline{v}^H \underline{x}_s)(X_o^* - \underline{x}_s^H \underline{v})] \\ &= E[|X_o|^2 - \underline{v}^H X_o^* \underline{x}_s - X_o \underline{x}_s^H \underline{v} + \underline{v}^H \underline{x}_s \ \underline{x}_s^H \underline{v}] \\ &= E[|X_o|^2] - \underline{v}^H E[X_o^* \underline{x}_s] - E[X_o \underline{x}_s^H]\underline{v} + \underline{v}^H E[\underline{x}_s \ \underline{x}_s^H]\underline{v}. \end{aligned} \tag{3.4}$$

The first term of (3.4) is the input signal power (interference + noise, because the desired signal is neglected). If the input interference power is taken as unity to normalize results to the input interference power, $E[|X_o|^2] = 1 + \sigma^2$, where σ^2 is the variance of the white Gaussian noise. Because the interference is uncorrelated with the noise, it is easily shown that $E[X_o^* \underline{x}_s] = \underline{d}_{iN}$ where $\underline{d}_{iN}$ is the steering vector in the direction of the interference. The subscript N denotes that the dimension of the steering vector is N-by-1, as opposed to (N+1)-by-1 in the MVB. The difference in dimension is because the steering vector is not applied to the auxiliary channel but only to subarray channels. The expected value of the outer product in the last term of (3.4) is the correlation matrix R:

$$R = E[\underline{x}_s \ \underline{x}_s^H]. \tag{3.5}$$

Its dimension is N-by-N because it correlates the subarray signals only; the auxiliary channel does not contribute to R. The rank of R is N due to the presence of the white Gaussian noise. It makes R non-singular and therefore invertible.

Now (3.4) can be written:

$$p_{res} = 1 + \sigma^2 - \underline{v}^H \underline{d}_{iN} - \underline{d}_{iN}^H \underline{v} + \underline{v}^H R \underline{v}. \tag{3.6}$$

The optimal subarray weight vector $\underline{v}_o$ is the one that minimizes the residual power. Minimization of the residual power is done by taking the derivative with respect to $\underline{v}^H$ and setting it to zero:

$$\begin{aligned} \frac{\delta p_{res}}{\delta \underline{v}^H} &= R\underline{v}_o - \underline{d}_{iN} = 0 \\ \underline{v}_o &= R^{-1} \underline{d}_{iN}. \end{aligned} \tag{3.7}$$

Using the matrix inversion lemma (2.16), the optimal subarray weight vector becomes:

$$\begin{aligned} \underline{v}_o &= \frac{1}{\sigma^2}(I - \frac{\underline{d}_{iN}\ \underline{d}_{iN}^H}{\sigma^2 + \underline{d}_{iN}^H \underline{d}_{iN}})\underline{d}_{iN} \\ &= \frac{1}{\sigma^2}(\underline{d}_{iN} - \frac{N\underline{d}_{iN}}{\sigma^2 + N}) \\ &= \frac{\underline{d}_{iN}}{\sigma^2 + N}. \end{aligned} \tag{3.8}$$

This weight vector, when applied to the subarray inputs, produces the minimum residual power after the subtraction from the auxiliary channel.

3.3 The Cancellation Property of a TAS Array

Following the procedure for the MVB, the cancellation property of a TAS array can be evaluated. The procedure calls for substituting the optimal subarray weight vector (3.8) in the expression for the residual power (3.6). At this point, no time delay is used in the auxiliary channel ($t_d = 0$). The cancellation will be investigated at the carrier frequency. If the optimal subarray weight vector is applied, the residual power is:

$$\begin{aligned} p_{res} &= 1 + \sigma^2 - \underline{v}^H \underline{d}_{iN} - \underline{d}_{iN}^H \underline{v} + \underline{v}^H R \underline{v} \\ &= 1 + \sigma^2 - \underline{d}_{iN}^H R^{-1} \underline{d}_{iN} \\ &= 1 + \sigma^2 - \underline{d}_{iN}^H \frac{1}{\sigma^2}(I - \frac{\underline{d}_{iN}\ \underline{d}_{iN}^H}{\sigma^2 + N})\underline{d}_{iN} \\ &= 1 + \sigma^2 - \frac{N}{N + \sigma^2}. \end{aligned} \tag{3.9}$$

Using the assumption that $\sigma^2 \ll 1$, the residual power is $p_{res} \approx \sigma^2$. and the interference cancellation property of TAS is evident. Residual undesired power is equal to the thermal noise. The entire interference signal is cancelled. The comparison with (2.24) shows that MVB provides better cancellation if the angle of the arrival is not extremely small. It was shown that for the MVB $p_{res} \approx \sigma^2/(N+1)$ is possible to achieve, where σ^2 is the variance of the thermal noise at each element. Therefore,

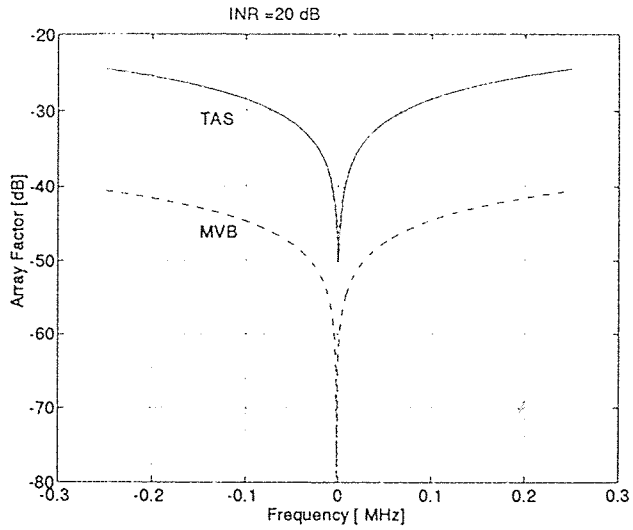

Figure 3.2 The array factor for the TAS without time delay.

the MVB is able to cancel more of the undesired signal than TAS without time delay ($t_d = 0$).

This conclusion can be illustrated with a numerical calculation of the array factor (frequency response in direction of the interference). In the TAS processor the array factor is given by:

$$A_{iTAS}(\omega) = |e^{-j\omega t_d} - \underline{v}_o^H \underline{d}_{iN}| \tag{3.10}$$

All array parameters are taken as in the numerical evaluation of the MVB (Figure 2.2). For TAS, Figure 3.2 is obtained. The array factor for the MVB is repeated on Figure 3.2 (dashed line). The corresponding TAS response is plotted using the full line. Better cancellation for the MVB can be observed from Figure 3.2. However this does not mean that the TAS array is inferior than the MVB. The main feature of TAS, the frequency compensation using time delay t_d, is not utilized if $t_d = 0$. It can be expected that using the compensation time delay t_d, the improvement in the array factor will be achieved. The question of the best choice for the time delay arises. This question is addressed in the next section.

3.4 The Optimal Time Delay

The optimal time delay must provide the least residual power after the TAS processing. The TAS processing includes weighting the N subarray input signals and time delaying the signal in the auxiliary channel. After subtraction of the subarray output from the auxiliary channel, low residual power is desired. The frequency interval considered must satisfy the narrowband criterion $Nd \ll c/B$ to enable the mathematical analysis. If the narrowband criterion holds, the optimal subarray weight vector can be calculated only at the carrier frequency. This weight vector can be then applied to a frequency interval B satisfying the criterion. If the bandwidth is taken symmetrically centered around the carrier, the problem can be defined: Minimize $p_{res} = \int_{-\Delta\omega/2}^{\Delta\omega/2} |w_o(\omega) - \underline{v}_o^H \underline{d}_{iN}(\omega)|^2 d\omega$. Symbol $\Delta\omega$ denotes the angular frequency interval in which the interference has non-zero spectral components. Coefficient w_o is equal to $e^{-j\omega t_d}$ and the optimal subarray weight vector $\underline{v}_o$ is given with (3.8). We first evaluate the inner product $\underline{v}_o^H \underline{d}_{iN}(\omega)$:

$$\begin{aligned} \underline{v}_o^H \underline{d}_{iN}(\omega) &= \frac{\underline{d}_{iN}^H}{\sigma^2 + N} \underline{d}_{iN}(\omega) \\ &= \frac{1}{\sigma^2 + N} \sum_{k=1}^{N} e^{-j\omega\tau_i k} \\ &= \frac{1}{\sigma^2 + N} e^{-j\omega\tau_i (N+1)/2} \frac{\sin(\omega\tau_i N/2)}{\sin(\omega\tau_i/2)}. \end{aligned} \tag{3.11}$$

To simplify further procedure, two substitutions are made:

$$\begin{aligned} a &= (N+1)\tau_i/2 \\ b(\omega) &= \frac{1}{\sigma^2 + N} \frac{\sin(N\omega\tau_i/2)}{\sin(\omega\tau_i/2)}. \end{aligned} \tag{3.12}$$

Using these substitutions, (3.11) becomes

$$\underline{v}_o^H \underline{d}_{iN}(\omega) = b(\omega) e^{-j\omega a}. \tag{3.13}$$

The expression for the total residual power now becomes

$$p_{res} = \int_{-\Delta\omega/2}^{\Delta\omega/2} |e^{-j\omega t_d} - b(\omega) e^{-j\omega a}|^2 d\omega. \tag{3.14}$$

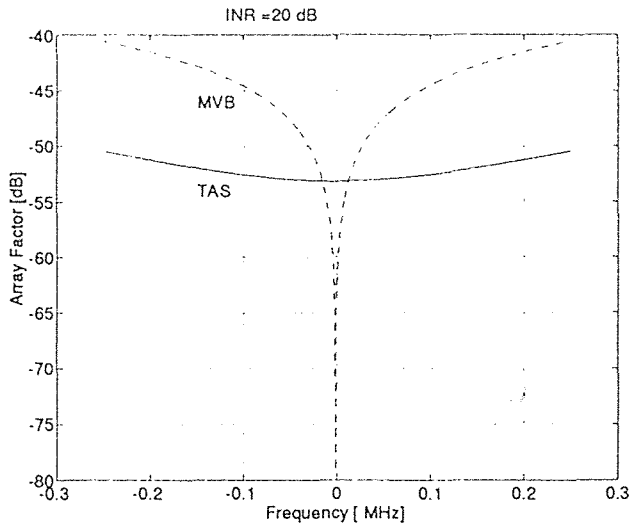

Figure 3.3 The array factor for TAS with the optimal time delay.

Further development of (3.14) gives:

$$p_{res} = \int_{-\Delta\omega/2}^{\Delta\omega/2} [1 - b(\omega)e^{j\omega(a-t_d)} - b(\omega)e^{-j\omega(a-t_d)} + b^2(\omega)]d\omega. \tag{3.15}$$

Integral (3.15) can be separated in two integrals:

$$p_{res} = \int_{-\Delta\omega/2}^{\Delta\omega/2} (1 + b^2(\omega))d\omega - \int_{-\Delta\omega/2}^{\Delta\omega/2} b(\omega)(e^{-j\omega(a-t_d)} + e^{j\omega(a-t_d)})d\omega. \tag{3.16}$$

Using the Euler's formula:

$$p_{res} = \int_{-\Delta\omega/2}^{\Delta\omega/2} (b^2(\omega) + 1)d\omega - 2\int_{-\Delta\omega/2}^{\Delta\omega/2} b(\omega)\cos[\omega(a - t_d)]d\omega. \tag{3.17}$$

The residual power will be the least possible when the second term is maximized. It is maximized when the argument of the cos function is zero, which leads to the optimality criterion $a = t_d$. Substituting (3.12) for a, the optimal time delay is:

$$t_{dopt} = (N + 1)\tau_i/2. \tag{3.18}$$

Using the optimal value for the compensation time delay t_d given with (3.18), the array factor (3.10) has been calculated. The result is shown in Figure 3.3.

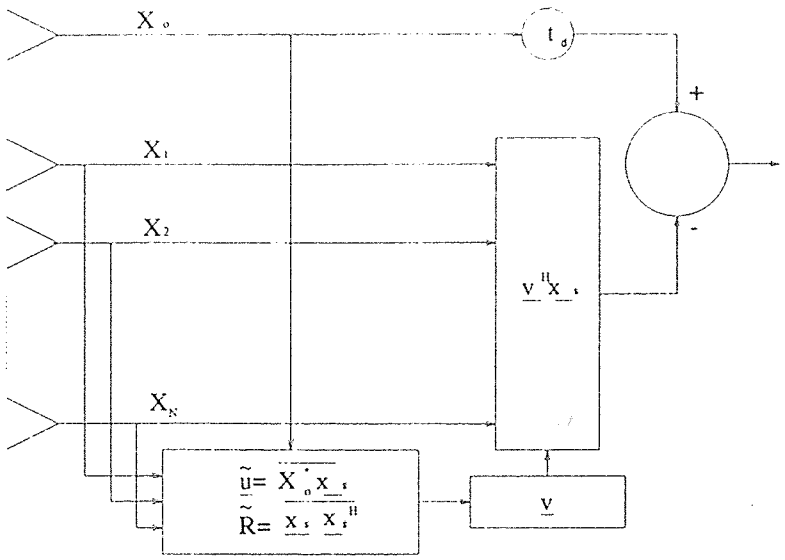

Figure 3.4 Block diagram of the TAS array implementation.

The comparison with the MVB (dashed line) shows that the objective is met. The frequency response is better than for the MVB. The improvement manifest itself in the smaller total area under the array factor curve. It means smaller gain in the direction of the interference inside the frequency interval under consideration (500 KHz).

The block diagram for the practical implementation of TAS is shown in Figure 3.4. Instead of the expectations that were used in the mathematical analysis, the estimations must be used in practice. The correlator module must estimate both the autocorrelation of the subarray signals $\tilde{R} = \overline{\underline{x}_s \, \underline{x}_s^H}$ and the cross-correlation vector $\underline{\tilde{u}} = \overline{X_o^* \underline{x}_s}$. The correlation matrix correlates the subarray inputs while the cross-correlation vector correlates the signal from the auxiliary channel (X_o) with the subarray input signals ($\underline{x}_s$). Further steps include the calculation of the weight vector using the estimated values, beamforming the subarray output and subtraction of the beamformed subarray output from the auxiliary channel output. The minimum

variance estimates are averages:

$$\begin{aligned} \overline{\underline{x}_s \ \underline{x}_s^H} &= \frac{1}{L}\sum_{l=1}^{L} \underline{x}_{sl} \ \underline{x}_{sl}^H \\ \overline{X_o^* \underline{x}_s} &= \frac{1}{L}\sum_{l=1}^{L} X_{ol}^* \underline{x}_{sl}. \end{aligned} \tag{3.19}$$

A set of the input signals is denoted as a snapshot. Subscript l denotes the l-th snapshot of the input data and L is the total number of snapshots that are used for the estimation.

To reiterate, the TAS array showed lower array factor than the MVB. However, the choice of the optimal time delay was essential. The improvement of TAS over the MVB was obtained only for the specific values of the compensation time delay (t_d) in the auxiliary channel. Therefore, the precise timing of sampling is important for TAS to achieve improvement over the MVB in terms of the gain in the direction of the interference.

3.5 The Optimal Weight Vector for a Deterministic Case

In this section, it is assumed that the direction of arrival of the interference is known. This situation is referred to as the deterministic case. In this case, the optimal subarray weight vector is calculated differently than in the adaptive case where the angle of arrival was unknown (3.7). Since the direction of the interference is known, the steering vector to the interference $\underline{d}_{iN}$ (2.5) can be used in calculations. For the adaptive case in the previous sections, the correlation matrix and the steering vector to the desired signal $\underline{d}_o$ were used to calculate the optimal subarray weight vector (3.7). In the deterministic case there is no need to use the correlation matrix. The knowledge of $\underline{d}_{iN}$ enables to minimize noise by minimizing the norm of the weight vector $\underline{v}$ using the appropriate constraints to prevent trivial solution $\underline{v}_o = \underline{0}$, where $\underline{0}$ denotes the null-vector. When this inner product ($\underline{v}^H \underline{v}$) is minimum, it will provide minimum thermal noise at the output. This holds for the Gaussian white noise for

which the output power is $\underline{v}^H N \underline{v}$. Since matrix N for the white noise is $\sigma^2 I$, where I is the identity matrix, the output noise simplifies to $\sigma^2 \underline{v}^H \underline{v}$.

The objective in the deterministic case can be stated:

$$\text{Minimize } \underline{v}^H \underline{v} \text{ subject to } \underline{v}^H \underline{d}_o = 0 \text{ and } \underline{v}^H \underline{d}_{iN} = 1.$$

The desired signal is cancelled at the output of the subarray. Therefore, the desired signal at the output of the TAS processor is provided by the auxiliary channel. The interference is passed at the output of the subarray with the unity gain. It is cancelled after the subtraction from the auxiliary channel output. The objective can be mathematically defined in the form of a cost function:

$$J = \underline{v}^H \underline{v} - \lambda_1 (\underline{v}^H \underline{d}_o - 0) - \lambda_2 (\underline{v}^H \underline{d}_{iN} - 1). \tag{3.20}$$

Minimizing J with respect to $\underline{v}^H$ amounts to taking the derivative and setting it to zero:

$$\begin{aligned} \frac{\delta J}{\delta \underline{v}^H} &= \underline{v} - \lambda_1 \underline{d}_o - \lambda_2 \underline{d}_{iN} = 0 \\ \underline{v} &= \lambda_1 \underline{d}_o + \lambda_2 \underline{d}_{iN}. \end{aligned} \tag{3.21}$$

Using the constraints, two linear equations for the Lagrange coefficients λ_1 and λ_2 are obtained:

$$\begin{aligned} \lambda_1^* \underline{d}_o^H \underline{d}_o + \lambda_2^* \underline{d}_{iN}^H \underline{d}_o = 0 \\ \lambda_1^* \underline{d}_o^H \underline{d}_{iN} + \lambda_2^* \underline{d}_{iN}^H \underline{d}_{iN} = 1. \end{aligned} \tag{3.22}$$

Solving this system gives:

$$\begin{aligned} \lambda_1^* &= \frac{\underline{d}_{iN}^H \underline{d}_o}{\underline{d}_{iN}^H \underline{d}_o \;\; \underline{d}_o^H \underline{d}_{iN} - \underline{d}_o^H \underline{d}_o \;\; \underline{d}_{iN}^H \underline{d}_{iN}} \\ \lambda_2^* &= \frac{\underline{d}_o^H \underline{d}_o}{\underline{d}_o^H \underline{d}_o \;\; \underline{d}_{iN}^H \underline{d}_{iN} - \underline{d}_{iN}^H \underline{d}_o \;\; \underline{d}_o^H \underline{d}_{iN}}. \end{aligned} \tag{3.23}$$

Steering vectors $\underline{d}_o$ and $\underline{d}_{iN}$ are under the narrowband assumption defined as:

$$\begin{aligned} \underline{d}_o^T &= [e^{-j\omega_c \tau_o} \ldots\ldots e^{-j\omega_c N \tau_o}] \\ \underline{d}_{iN}^T &= [e^{-j\omega_c \tau_1} \ldots\ldots e^{-j\omega_c N \tau_1}]. \end{aligned} \tag{3.24}$$

Since the desired signal is assumed to arrive delay-free, $\underline{d}_o$ is the vector of ones. Using (3.24), the inner products in (3.23) can be explicitly calculated:

$$\begin{aligned} \underline{d}_o^H \underline{d}_0 &= \underline{d}_{iN}^H \underline{d}_{iN} = N \\ \underline{d}_o^H \underline{d}_{iN} &= e^{-j\omega_c \tau_i (N+1)/2} \frac{\sin(\omega_c \tau_i N/2)}{\sin(\omega_c \tau_i/2)} \\ \underline{d}_{iN}^H \underline{d}_o &= e^{j\omega_c \tau_i (N+1)/2} \frac{\sin(\omega_c \tau_i N/2)}{\sin(\omega_c \tau_i/2)}. \end{aligned} \tag{3.25}$$

Denoting

$$\underline{d}_o^H \underline{d}_{iN} = s, \tag{3.26}$$

the Lagrange coefficients become:

$$\begin{aligned} \lambda_1 &= \frac{s^*}{|s|^2 - N^2} \\ \lambda_2 &= \frac{N}{N^2 - |s|^2}. \end{aligned} \tag{3.27}$$

The final expression for the optimal subarray weight vector is:

$$\underline{v}_o = \frac{s^*}{|s|^2 - N^2} \underline{d}_o + \frac{N}{N^2 - |s|^2} \underline{d}_{iN}. \tag{3.28}$$

Using the optimal subarray weight vector defined at (3.28), the output is obtained by subtracting the beamformed subarray output from the auxiliary channel output:

$$Y(\omega) = X_o(\omega) e^{-j\omega t_d} - \underline{v}_o^H \underline{x}(\omega), \tag{3.29}$$

where $X_o(\omega)$ is the signal in the auxiliary channel and the exponential factor describes its time delay. The optimal time delay is (N+1)$\tau_i/2$ as is in the adaptive case (3.18).

The deterministic case could appear in practice if the angle of arrival of the interference is detected before the cancellation. Than the optimal subarray weight vector would be calculated using (3.28).

3.6 The Modular TAS

In this section an interesting issue in the TAS processing is addressed. A way of further improvement of the TAS performance is to repeat the procedure on more

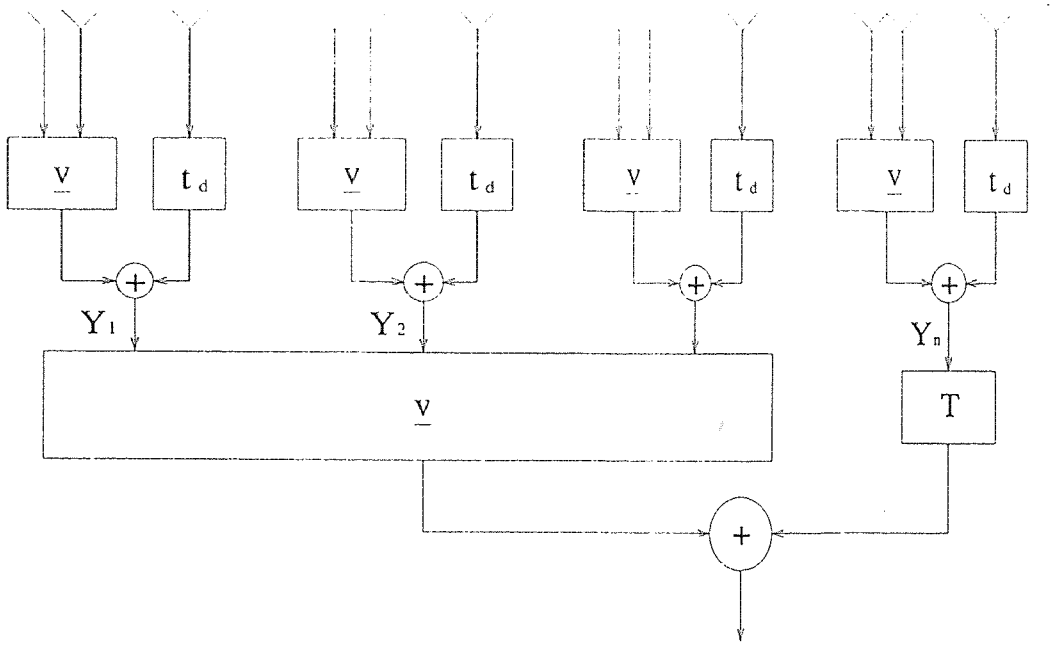

Figure 3.5 The two-level TAS processor.

than one level. In order to do so, the initial array is partitioned into modules. The configuration is shown on Figure 3.5. Outputs of each module can be further combined into higher order modules. The control of the sampling (denoted by t_d) is done on the first level at the each module. At the other levels, the time delay is implemented using a delay line (denoted by T). This is because the received signal is already sampled at the first level so we can not control the sampling in further levels.

The particular case will consider the three-element modules. The deterministic case covered in the previous section will be assumed. If the total number of sensors in the array is a multiple of three, the array can be partitioned into three-element modules. The configuration of one such module is shown in Figure 3.6. Results for the optimal subarray weight vector from the previous section can be readily applied to calculate the module array factor (gain in the direction of the interference). For a

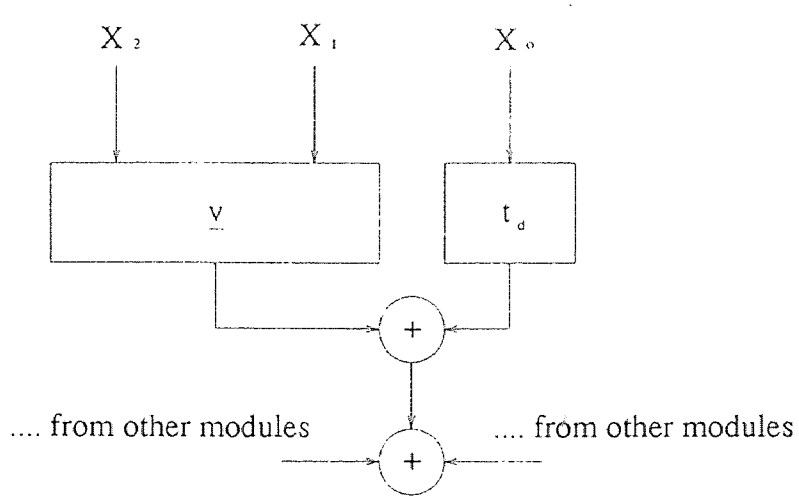

Figure 3.6 A three-channel module.

three-element array, N=2 (number of elements in the subarray) and (3.25) becomes:

$$\begin{aligned} \underline{d}_o^H \underline{d}_o &= 2 \\ |s| &= \frac{\sin(\omega_c \tau_i)}{\sin(\omega_c \tau_i/2)} = 2\cos(\omega_c \tau_i/2). \end{aligned} \tag{3.30}$$

The optimal subarray weight vector becomes:

$$\underline{v}_o = -\frac{2e^{3j\omega_c \tau_i/2}\cos(\omega_c \tau_i/2)}{4\sin^2(\omega_c \tau_i/2)}\underline{d}_o + \frac{2}{4\sin^2(\omega_c \tau_i/2)}\underline{d}_{iN}. \tag{3.31}$$

Steering vectors are simple due to only two subarray elements:

$$\begin{aligned} \underline{d}_o^T &= [1 \quad 1] \\ \underline{d}_{iN}^T &= [e^{-j\omega_c \tau_i} \quad e^{-j\omega_c 2\tau_i}]. \end{aligned} \tag{3.32}$$

The array factor to the interference (i.e. the gain in the direction of the interference) for a single module is calculated by subtracting the subarray output from the auxiliary channel output. The expression is given with (3.10) but the optimal subarray weight vector given with (3.31) must be used because the deterministic case is assumed. To obtain the final array output, all module outputs are added. These module outputs are denoted with $Y_1 \cdots Y_n$ in Figure 3.5. The result of this addition

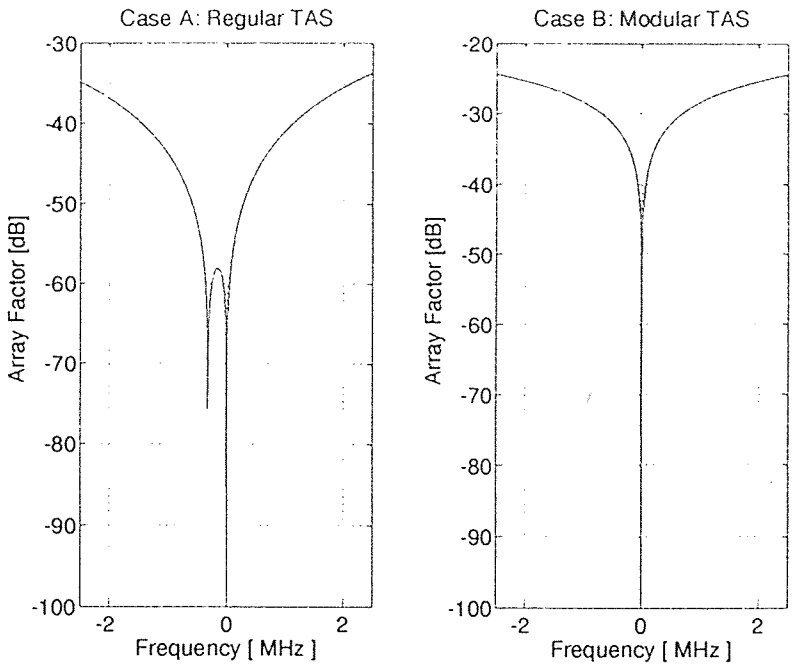

Figure 3.7 The array factor for one-level modular TAS.

is shown in Figure 3.7. This result is obtained using 15 elements in the initial array. The angle of arrival of the interference is taken as 60^o. Carrier frequency of 1 GHz is assumed. The array factor is calculated for the interference bandwidth of 5 MHz, which satisfies the narrowband criterion (percentage bandwidth is 0.5 % relative to the carrier). On the plot denoted "Case A", the regular TAS processing result is shown. The processing is done on the entire array. The optimal time delay is used (for 15-element array the optimal compensation time delay is $t_d = 7.5\tau_j$). Plot denoted "Case B" presents result when the array is partitioned in five 3-element modules. In each module regular TAS processing is performed using the optimal time delay $t_d = \frac{3}{2}\tau_i$. Outputs from all the modules ($Y_1 \cdots Y_n$ in Figure 3.5) are added without additional processing. It can be seen that the case A is better in the sense that it provides smaller gain in the direction of interference across the frequency band of interest. So, simple superposition of the module outputs (B) is not enough

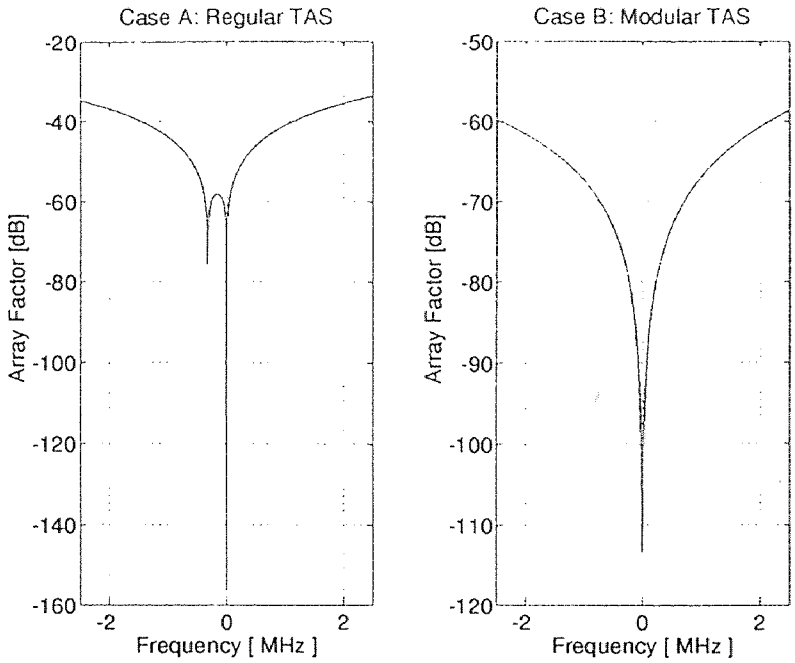

Figure 3.8 The array factor for two-level modular TAS.

to improve the performance of the TAS structure over the case of non-partitioned array (A).

The next step was an attempt to use module outputs as inputs to a new, second level, TAS processor. This procedure is shown on Figure 3.5. For the observed case of 15 initial elements, this would lead to 4 elements in the subarray plus an auxiliary channel. Applying the TAS method at this point requires propagation time delay of $3\tau_i$ to be used. This is because a three-element module has time delay three times the original propagation delay among neighbouring elements. The compensation time delay is denoted with T in Figure 3.5 and can not be realized with the control of sampling because sampling is already done at the first level. Rather a time delay line is used in higher levels.

Results of the second level TAS processing are plotted on the Figure 3.8. The array factor is calculated as a function of frequency using (3.10) and the optimal

subarray weight vector given with (3.31). The regular TAS processing (without partitioning) is presented again for convenience (case A). Case B is the plot of the final output. It can be seen that in case B, the array factor is lower which means that the array will provide more attenuation in the interference direction than one-level TAS (case A).

To reiterate, simple superposition of the module-outputs is not enough to improve the cancelling ability of a TAS processor compared to the non-partitioned array. The solution is to apply the time delay T on the output of one of the modules. The outputs from other modules become inputs to a next level subarray. Apparently, more such steps are possible. Grouping first level modules in second level and so forth, would lead to the further increase in the level of the interference cancellation.

This extension of TAS serves primarily as a theoretical concept. It is likely to suffer from the increased hardware complexity. However, it offers potentials to obtain very good results in the interference cancellation and could be a subject of a separate research.

CHAPTER 4

WIDEBAND INTERFERENCE CANCELLATION

4.1 Introduction

In the approach taken so far, a narrowband interference signal was assumed. The correlation matrix was obtained as the sum $R = R_i + R_n$, where R_i denotes the interference correlation matrix and R_n denotes the thermal noise correlation matrix. The matrix R_i was obtained as an outer product of the steering vectors: $R_i = p_i \underline{d}_i \underline{d}_i^H$, where p_i is the total interference power at the input. The steering vectors were calculated only at the carrier frequency. Thermal noise was modelled as white noise (white in space) with the power level σ^2. For a wideband interference signal, the noise is modelled as white Gaussian both in space and in frequency, because now a frequency interval is observed rather than a single frequency. Therefore, the noise correlation matrix is $R_n(\omega) = \sigma_d^2 I$ at every frequency in the interval, where σ_d^2 denotes the power spectral density of the noise. In the wideband case, $R_i = p_i \underline{d}_i \ \underline{d}_i^H$ can not be taken if the interference has frequency components far from the carrier frequency. The criterion for checking whether this dyadic form can be used is $Nd \ll c/B$ as stated in the Chapter 2. If the bandwidth B is large so this criterion is not fulfilled, the interference correlation matrix must be calculated over all frequencies at which signal has non-zero spectrum. The calculation of this correlation matrix is presented in the next section followed by the calculation of the optimal weight vector and the output power.

4.2 Wideband Interference Correlation Matrix

The correlation matrix will be calculated in this section for the interference that has flat spectrum centered around the carrier. Under this assumption the power spectral density is at every frequency $S(\omega) = p_i/\Delta\omega$, where p_i is total interference power at

the input and $\Delta\omega$ is the bandwidth in the baseband. The array input can be written in a vector form as:

$$\underline{x}(\omega) = X(\omega)\underline{d}_i(\omega) + \underline{n}(\omega), \tag{4.1}$$

where $\underline{d}_i(\omega)$ is the steering vector in the interference direction defined with (2.5) and $\underline{n}(\omega)$ is the vector of noise components. The correlation matrix for the input vector $\underline{x}(\omega)$ is defined as an integral over the entire frequency band:

$$R_w = E[\int_{-\Delta\omega/2}^{\Delta\omega/2} \underline{x}(\omega)\ \underline{x}^H(\omega)d\omega], \tag{4.2}$$

where subscript w denotes wideband interference. Substituting (4.1) in (4.2) gives:

$$R_w = E\int_{-\Delta\omega/2}^{\Delta\omega/2} (X(\omega)\underline{d}_i(\omega) + \underline{n}(\omega))(X^*(\omega)\underline{d}_i^H(\omega) + \underline{n}^H(\omega))d\omega. \tag{4.3}$$

Additive noise is a zero-mean Gaussian process with the variance σ^2 and is uncorrelated with the interference signal:

$$R_w = \int_{-\Delta\omega/2}^{\Delta\omega/2} E[|X(\omega)|^2]\underline{d}_i(\omega)\ \underline{d}_i^H(\omega)d\omega + \int_{-\Delta\omega/2}^{\Delta\omega/2} E[\underline{n}(\omega)\ \underline{n}^H(\omega)]d\omega. \tag{4.4}$$

Using the assumption that the power spectral density is constant, the expectations in (4.4) are not functions of frequency and the correlation matrix becomes:

$$R_w = \int_{-\Delta\omega/2}^{\Delta\omega/2} \frac{p_i}{\Delta\omega}\underline{d}_i(\omega)\ \underline{d}_i^H(\omega)d\omega + \int_{-\Delta\omega/2}^{\Delta\omega/2} \sigma_d^2 I\, d\omega, \tag{4.5}$$

where σ_d^2 is the noise power spectral density: $\sigma_d^2 = \frac{\sigma^2}{\Delta\omega}$. The outer product of the steering vectors is:

$$\underline{d}_i(\omega)\ \underline{d}_i^H(\omega) = [e^{-j(\omega_c+\omega)\tau_i} \cdots e^{-jN(\omega_c+\omega)\tau_i}]^T\ \ [e^{j(\omega_c+\omega)\tau_i} \cdots e^{jN(\omega+\omega_c)\tau_i}], \tag{4.6}$$

where ω_c denotes the carrier angular frequency and ω denotes the baseband frequency of the interference. The outer product (4.6) results in a matrix $M(\omega)$ whose elements m are of the form:

$$m_{r,c}(\omega) = e^{j(\omega+\omega_c)\tau_i(r-c)}, \tag{4.7}$$

where r denotes the row and c denotes the column of the matrix $M(\omega)$. Correlation matrix is now:

$$R_w = \frac{p_i}{\Delta\omega}\int_{-\Delta\omega/2}^{\Delta\omega/2} M(\omega)d\omega + \sigma^2 I. \tag{4.8}$$

Integrating terms such as shown by (4.7) gives the terms of the correlation matrix R_w:

$$R_{w(r,c)} = \frac{p_i}{\Delta\omega}e^{j\omega_c\tau_i(r-c)}\frac{e^{j\omega(r-c)\tau_i}}{j\tau_i(r-c)}|_{-\Delta\omega/2}^{\Delta\omega/2} + \sigma^2\delta(r,c), \tag{4.9}$$

where $\delta(r,c)$ is the Kronecker delta and is defined as:

$$\delta(r,c) = \begin{cases} 1 & \text{if r = c} \\ 0 & \text{otherwise} \end{cases} \tag{4.10}$$

Using the Euler formula, the elements of the correlation matrix finally become:

$$R_{w(r,c)} = p_i e^{-j\omega_c(r-c)\tau_i}\frac{sin(\Delta\omega(r-c)\tau_i/2)}{\Delta\omega(r-c)\tau_i/2} + \sigma^2\delta(r,c). \tag{4.11}$$

The narrowband criterion $Nd \ll c/B$ can be understood from (4.11). In order to approximate (4.11) with the expression for the narrowband correlation matrix, sinc $(\sin(x)/x)$ term must be close to one. If this holds, (4.11) simplifies to $R_{w(r,c)} = p_i e^{-j\omega_c(r-c)\tau_i} + \sigma^2\delta(r,c)$. This is the expression for the narrowband correlation matrix where everything is observed at the carrier frequency. Further development of the condition that sinc term is close to unity would give the narrowband criterion $Nd \ll c/B$. Under this criterion, (4.11) can be written without the sinc term and matrix R_w is analytically invertible using the matrix inversion lemma (2.16).

Two facts can be observed from (4.11). If σ^2 is finite, R_w will be non-singular. This always holds in practice due to the unavoidable presence of additive noise. Second fact is inability to express matrix R_w in a form of a sum of two matrices A+B, where A is a nonsingular matrix and B is a dyadic form (i.e. an outer product of vectors). Because of this, the matrix inversion lemma ([12]) can not be used. This makes the retrieval of the analytical results difficult. In the case of a narrowband interference, the correlation matrix could have been inverted analytically while in

the case of a wideband interference, numerical methods must be used to calculate the optimal weight vector.

4.3 Calculation of the Optimal Weight Vector

The correlation matrix calculated in the previous section will be used to calculate the optimal weight vector. The optimal weight vector in the MVB ($\underline{w}_o$) is the solution of the optimization problem: Minimize residual power subject to constraint $\underline{w}_o^H \underline{d}_o = 1$. The residual power is given with $p_{res} = \underline{w}^H R_w \underline{w}$. Solving this optimization problem gives for the optimal weight vector:

$$\underline{w}_o = \frac{R_w^{-1} \underline{d}_o}{\underline{d}_o^H R_w^{-1} \underline{d}_o}. \tag{4.12}$$

This is the same as (2.19) except for the usage of the wideband correlation matrix R_w. Because of inability to analytically invert this matrix, the numerical solution for $\underline{w}_o$ must be found.

For TAS, the objective is to minimize the output power in the entire frequency range. The output power is the residual after subtracting the subarray output from the auxiliary channel output. The residual power is:

$$p_{res} = E[\int_{-\Delta\omega/2}^{\Delta\omega/2} |X_o(\omega) e^{-j\omega t_d} - \underline{v}^H \underline{x}_s(\omega)|^2 d\omega], \tag{4.13}$$

where $X_o(\omega)$ is the signal in the auxiliary channel, the exponential term represents the compensation time delay in the frequency domain, $\underline{v}$ is the subarray weight vector, and $\underline{x}_s(\omega)$ is the subarray input vector. Expanding (4.13) will produce four terms:

$$p_{res} = p_o - \underline{v}^H \underline{u} - \underline{u}^H \underline{v} + \underline{v}^H R_w \underline{v}. \tag{4.14}$$

Developing (4.13), it can be easily shown that the first term is:

$$p_o = \int_{-\Delta\omega/2}^{\Delta\omega/2} |X_o(\omega)|^2 d\omega = p_i + \sigma^2. \tag{4.15}$$

Vector $\underline{u}$ which comes in two middle terms is defined as:

$$\underline{u} = E[\int_{-\Delta\omega/2}^{\Delta\omega/2} X_o^*(\omega) e^{j\omega t_d} \underline{x}_s(\omega) d\omega, \tag{4.16}$$

where $\underline{x}_s(\omega)$ is the subarray input vector. After some simple manipulations, the cross-correlation vector $\underline{u}$ becomes:

$$\underline{u} = \int_{-\Delta\omega/2}^{\Delta\omega/2} \underbrace{\frac{p_i}{\Delta\omega} e^{j\omega t_d} \underline{d}_i(\omega)}_{\underline{q}} d\omega \,. \tag{4.17}$$

The expression under the integral is vector $\underline{q}$ whose k-th component is:

$$q_k = e^{j\omega t_d} e^{-j(\omega+\omega_c)\tau_i k}. \tag{4.18}$$

Integration of a such term gives finally for the k-th element of the cross-correlation vector $\underline{u}$:

$$u_k = p_i e^{-j\omega_c \tau_i k} \frac{sin(\Delta\omega(t_d - \tau_i k)/2)}{\Delta\omega(t_d - \tau_i k)/2}. \tag{4.19}$$

The significant point of this derivation is the appearance of the compensation time delay in the expression for the wideband cross-correlation vector $\underline{u}$. Because of this, the optimal subarray weight vector depends on the compensation time delay.

The last term in (4.14) contains the subarray correlation matrix R_w. The components of the matrix R_w are given with (4.11). The correlation matrix appearing in (4.14) is N-by-N as opposed to (N+1)-by-(N+1) in the MVB case (4.12). This concludes the definition of the terms in (4.14).

The minimization of the residual power (4.13) defines the optimal subarray weight vector:

$$\begin{aligned} \frac{\delta p_{res}}{\delta \underline{v}^H} = 0 \Rightarrow R_w \underline{v}_o &= \underline{u} \\ \underline{v}_o &= R_w^{-1} \underline{u}. \end{aligned} \tag{4.20}$$

Since the compensation time delay t_d appears in the expression for $\underline{u}$, the optimal weight vector $\underline{v}_o$ will depend on the compensation time delay t_d. As was the case for

the MVB, the inability to invert the wideband correlation matrix R_w forces usage of numerical methods in calculating the optimal subarray weight vector.

Using the optimal subarray weight vector (4.20) and substituting (4.15) into (4.14), the residual power becomes:

$$p_{res} = p_i + \sigma^2 - \underline{u}^H R_w^{-1} \underline{u}. \tag{4.21}$$

The expression (4.21) calculates the residual power after TAS processing using the optimal subarray weight vector (4.20). For a flat interference, this calculation can be done using (4.11) for R_w and (4.19) for $\underline{u}$. If the frequency spectrum is arbitrary, the integral (4.8) for R_w and the integral (4.17) for $\underline{u}$ must be numerically evaluated. This is because the assumption that the interference spectrum is flat, enabled the analytical integration of (4.8) and (4.17).

4.4 Numerical Results

Using the expressions derived in previous sections, the residual interference power and the total residual power (interference+noise) can be calculated. In this section the expressions are calculated for the particular cases of array parameters. The calculation is done using the idealized signal model. The interference is assumed flat in the frequency region of interest. The expressions for the correlation matrix (4.11) and for the cross-correlation vector (4.19) are used. These expressions are obtained integrating (4.8) and (4.17) which can be done analytically for a flat interference. The effects of the bandwidth, the noise power, and the time delay are investigated. Some characteristic results are plotted. Results are chosen to represent realistic cases. Therefore, the bandwidths are limited to 20 % percentage bandwidth relative to the carrier and the input interference-to-noise ratio is limited to 20 dB. A 16-element antenna array is assumed operating on the carrier frequency of 1 GHz. These parameters are chosen to represent the AEW Radar.

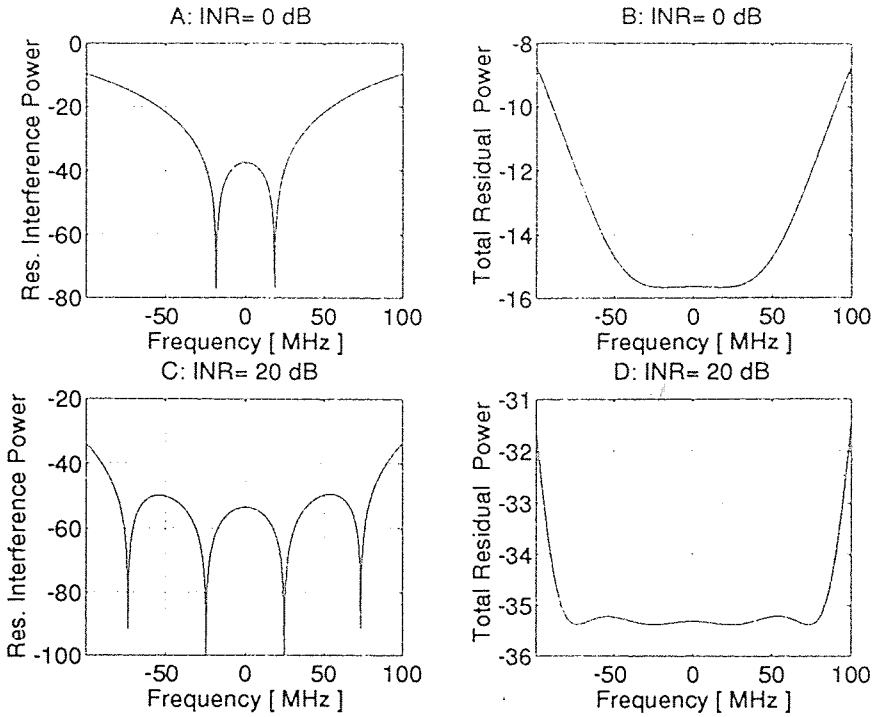

Figure 4.1 The effect of INR on the TAS cancellation.

Figure 4.1 shows the effect of the input noise level on the residual interference power and the total (interference+ noise) residual power. The result is calculated for the wideband case of 20 % fractional bandwidth (200 MHz centered around 1 GHz carrier). A 16-element TAS array was used with the optimal compensation time delay $t_d = 8\tau_i$ as calculated in Chapter 3. Sub-plots A and B are showing the case when the power levels of the interference and additive noise are of the same level at the input (INR=0 dB). Residual spectra of the interference only (A) and of the interference+noise (B) are shown. Residual powers are calculated as numerical integrals over the frequency band (i.e. areas under the curves). These powers are given with the expression (4.21). For the cases A and B these powers are 13 dBw for the interference residual power and 30.5 dBw for the total residual power (interference+noise). The unit dBw is decibels with respect to 1 microwatt. This

unit is chosen arbitrary and represents 1024 samples in the frequency domain that are assumed to be constant (1 microwatt) at each frequency. Therefore, the input interference power is 1024 microwatts $\approx$ 30 dBw. Therefore, the cancellation of the total residual power is only 2.5 dBw (the input interference power is 30 dBw and the interference to noise ratio is 0 dB,so the interference+noise power at the input is 30+3=33 dBw; 33-30.5=2.5 dBw). The cancellation of the interference is 30-13=17 dBw. So, the interference is attenuated 30.5-13=17.5 dB with respect to thermal noise at the output.

As expected, the increase in the interference input power relative to the noise makes the cancellation better. Sub-plots C and D show the residual spectra for INR=20 dB at the input. The residual interference power is reduced to -14 dBw which means that the cancellation is 44 dBw. The total residual power is $\approx$ 11 dBw which means that the cancellation is 30-11$\approx$19 dBw. The interference contributes less than 1 percent of the total (interference+noise) residual power (more than 20 dBw difference between the residual interference power and the total residual power). This illustrates the power inversion property of TAS: As the interference power is increased at the input (relative to the noise), better cancellation at the output is achieved.

Figure 4.2 shows how the bandwidth of the interference affects the performance of the TAS array. The case of INR=20 dB at the input is considered. Sub-plots A and B show the frequency spectra for a wideband case. The fractional bandwidth of 20 % relative to the carrier is assumed (200 MHz around 1 GHz carrier). This scenario is the same as on sub-plots C and D in Figure 4.1. Sub-plots C and D represent the narrowband case as can be seen from the abscissa. The fractional bandwidth is 0.5 % relative to the carrier. The same input interference power (30 dBw) is used for both bandwidths. This power is spread uniformly over the bands. Curves show the power spectra of the interference and interference+noise at the output. If the areas

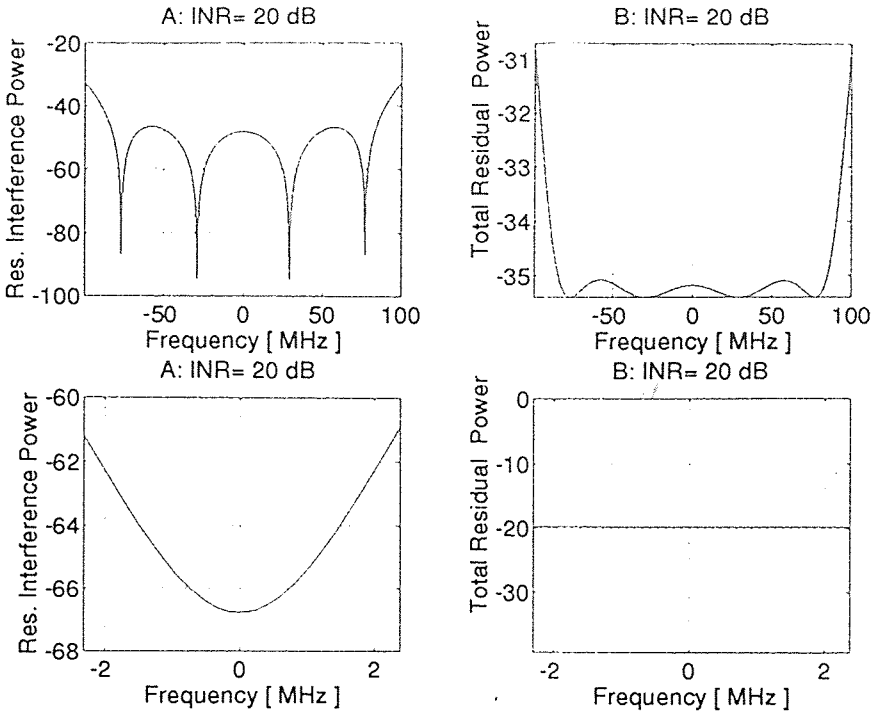

Figure 4.2 The effect of the bandwidth on the cancellation.

under the curves are calculated (this is same as calculating (4.21)), the results are as follows: When the fractional bandwidth is 20 % (A and B), the interference residual power (the area under the curve A) is -14 dBw. Since the interference was modelled to have 30 dBw input power, the cancellation is 44 dBw. The total residual power is $\approx$ 11 dBw (sub-plot B). If the same power is "compressed" to occupy narrower band, this will result in the significant improvement in the interference cancellation. For this case (sub-plot C), the residual interference power is as low as -34 dBw which means cancellation of 64 dBw. The improvement in the total residual power (interference+noise) is not as near so good. The total residual power is 10 dBw which means that the interference is completely covered inside the noise at the output (the interference power is 44 dBw less than the total residual power: 10-(-34)=44 dBw). So the main conclusion from the Figure 4.2 is the fact that if the interference

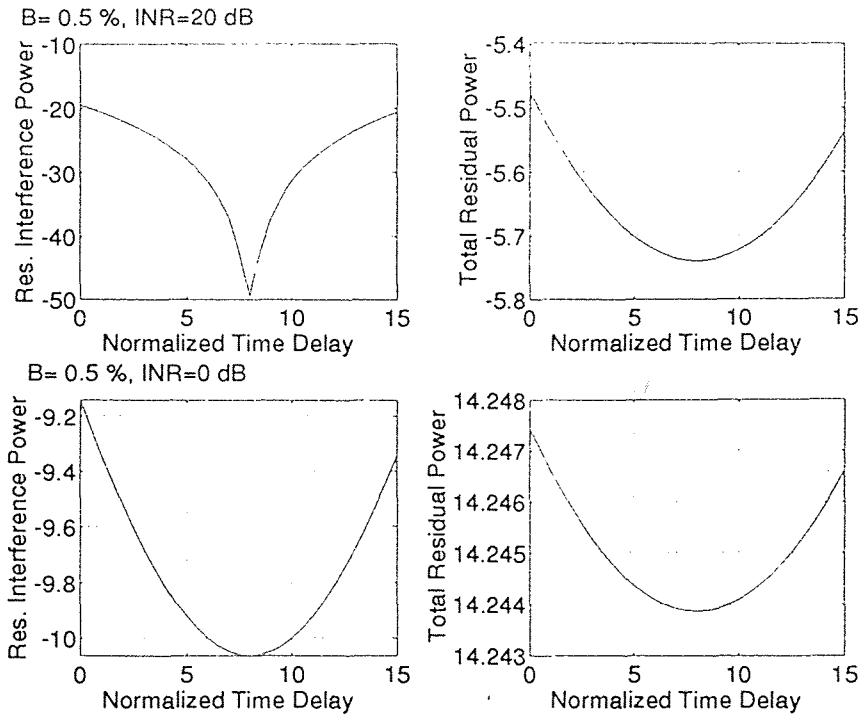

Figure 4.3 The effect of the INR on the effectivity of the time delay.

occupies narrower frequency interval, the better cancellation is achievable than for the interference of the same input power but spread over a wider interval.

Figure 4.3 shows how the noise level at the array input affects the effectivity of the compensation time delay. The same plot can serve to graphically illustrate the result from Section 3.4 for the optimal compensation time delay. In that section it was analytically shown that the optimal time delay to be applied in the auxiliary channel is $(N+1)\tau_i/2$, where (N+1) is the number of elements in the array and τ_i is the propagation time delay between the two consecutive elements. Figure 4.3 is obtained for a 16 element array which, according to the formula (3.18), has the best cancellation for $t_d = 8\tau_i$. This can be seen from the figure. The abscissa (compensation time delay t_d) is normalized to the propagation time delay τ_i, so the normalized time delay is t_d/τ_i. The other conclusion drawn from this figure

is that the increase in the noise level at the input (relative to the interference), decreases the effectivity of the compensation time delay. If noise has significant power (INR=0 dB; sub-plots C and D), the residual power of both the interference and the interference+noise (total residual power) depend very little on the compensation time delay t_d applied. If INR is 20 dB (sub-plots A and B), it results in the enhanced effectivity of the compensation time delay compared with the INR=0 dB case. This is obvious for the residual interference power (sub-plot A) which differs as much as $\approx$ 30 dB between the optimal time delay ($t_d = 8\tau_i$) and no time delay at all. The total residual power (sub-plot B) shows less dependence on the time delay, due to the fact that the compensation time delay affects mainly the directional interference. Residual noise power is determined by the gain which is equal to the norm of the weight vector and is unaffected with the compensation time delay. The noise power dominates in the total residual power (interference+noise), so the time delay does not affect the total residual power. Therefore, we can expect that the compensation time delay will have more effect as noise is decreased relative to the interference.

Figure 4.4 shows how the compensation time delay works for different interference bandwidths. The cases of fractional bandwidths of B=0.5 % and B=20 % are compared. For the fractional bandwidth B=0.5 % (sub-plots A and B), the sub-plots A and B from Figure 4.3 are repeated for convenience. Sub-plots C and D show the effectivity of the compensation time delay for the case of B=20 %. Multiple minima appear for the residual interference power. That means there are more than one optimal time delay t_d that produce minimum interference at the output. The appearance of the additional minima is attributed to the periodicity of the trigonometric functions which build the expressions for optimal weight vectors. If the frequency bandwidth is significant, the arguments of the trigonometric functions (of the form $\Delta\omega t_d$) will occupy interval larger than 2π. Therefore, the same residual interference power is obtained for $\Delta\omega t_{d1}$ and for $\Delta\omega t_{d2}$, where $\Delta\omega t_{d2} = \Delta\omega t_{d1} + 2\pi$.

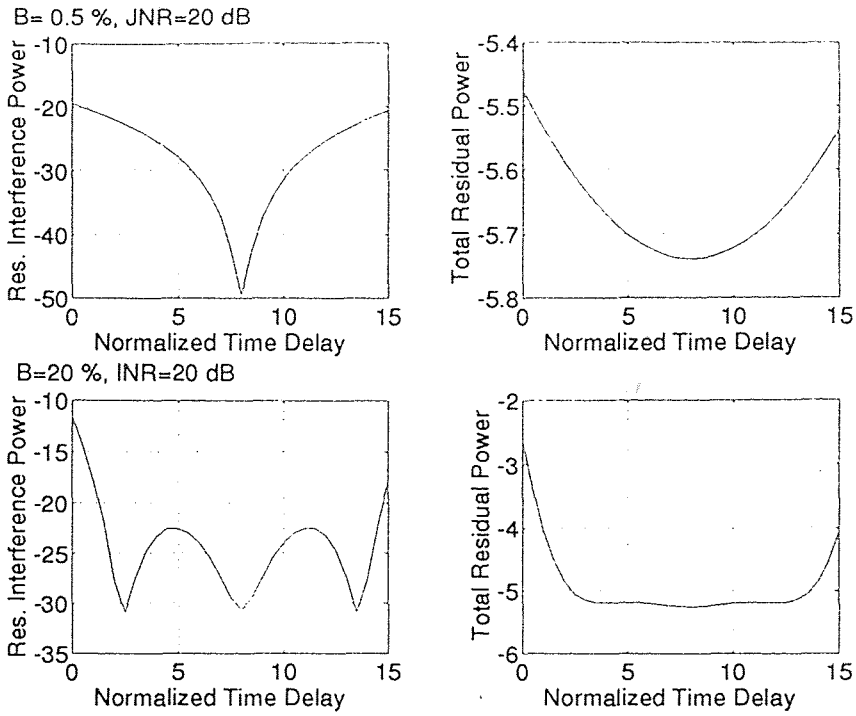

Figure 4.4 The effect of the bandwidth on the effectivity of the time delay.

Residual interference+noise power (sub-plot D) is almost constant for the wide interval of the compensation time delays, as discussed in connection with Figure 4.3.

4.5 The Comparison Between TAS and the MVB

Factors that affect the performance of TAS are considered in the previous section. A brief comparison with the MVB will be given in this section. The wideband interference correlation matrix (4.11) is used to calculate the optimal weight vectors.

For the MVB, the array factor is given as:

$$A_{iMVB}(\omega) = |\underline{w}_o^H \underline{d}_i(\omega)|, \tag{4.22}$$

where subscript i denotes that the array factor is calculated in the direction of the interference. Vectors $\underline{w}_o$ and $\underline{d}_i(\omega)$ are the optimal weight vector (4.12) and the

steering vector in the direction of the interference, respectively. The optimal weight vector does not depend on frequency. However, it is calculated using the wideband correlation matrix (4.11) and therefore will be optimal for the given frequency range.

For the TAS processor, the array factor is given as:

$$A_{iTAS}(\omega) = |e^{-j\omega t_d} - \underline{v}_o^H \underline{d}_i(\omega)|, \tag{4.23}$$

where the exponential term represents the time delay in the auxiliary channel and $\underline{v}_o$ is the optimal subarray weight vector given with (4.20). But in order to compare the MVB and TAS, the equivalent gain in the direction of the desired signal must be provided. Therefore, a constraint must be applied while calculating the subarray optimal weight vector. This constraint must ensure that the gain in the direction of the desired signal is unity. (4.20) is modified to:

$$\underline{v}_o = R_w^{-1}\underline{u} - \frac{(u^H R_w^{-1}\underline{d}_o)^H}{(\underline{d}_o^H R_w^{-1}\underline{d}_o)} R_w^{-1}\underline{d}_o. \tag{4.24}$$

The expression (4.24) is derived using the Lagrange coefficient method together with the constraint $\underline{v}^H\underline{d}_o = 0$. This constraint will null the desired signal at the subarray output. Therefore, the desired signal is supplied only by the auxiliary channel. Since the auxiliary channel is only time delayed, it will provide unitary gain in the direction of the desired signal. All results are calculated for a 16-element array and the carrier frequency $f_c = 1$ GHz.

The array factor defined in (4.22) and (4.23) will show the the gain in the direction of the interference as a function of frequency. This performance criterion is expected to be affected by the compensation time delay t_d in the auxiliary channel. Total residual power (interference+noise) is almost unaffected by t_d. The MVB has advantages over TAS in terms of total residual power. The reason is averaging thermal noise across the MVB array while the auxiliary channel in TAS passes the noise with the gain of unity. Thermal noise dominates at the output (interference is

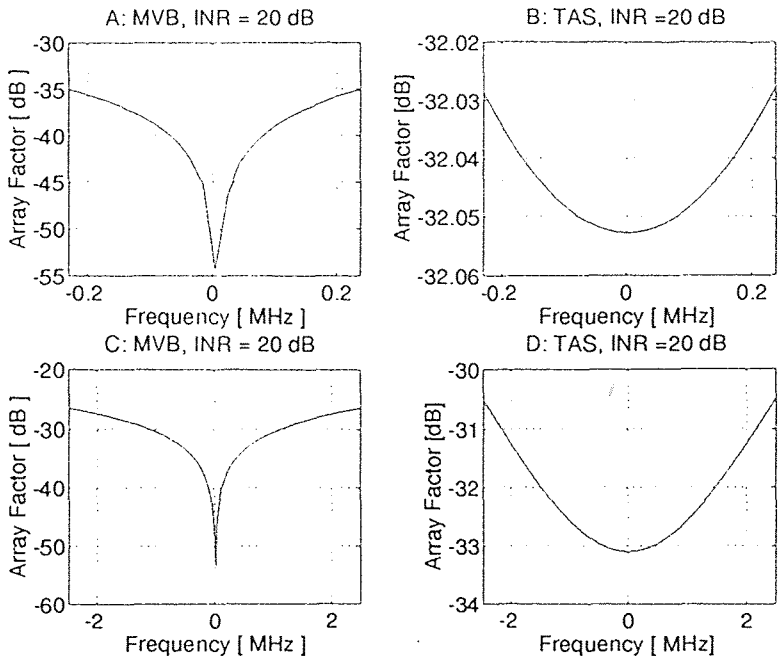

Figure 4.5 A comparison between MVB and TAS.

significantly cancelled by both the MVB and the TAS processor) and therefore the total residual power is less for the MVB.

Figure 4.5 compares the MVB and TAS for different bandwidths. All sub-plots are given for the INR=20 dB. Sub-plot A shows the array factor for the MVB (4.22) and the fractional bandwidth 0.05 %. Sub-plot B shows the corresponding TAS array factor (4.23). If the total array factor is calculated (integral of the array factor over all frequencies), the result shows less total array factor in the MVB case. It can be observed from the sub-plot B that TAS gives the array factor which is practically constant with respect to frequency (differences are 1/100 of a dB). If the fractional bandwidth is increased to 0.5 % the array factors plotted on the sub-plots C and D are obtained. If now the integral of the array factor is calculated over all frequencies, the TAS shows improvement over the MVB. The improvement is in the fact that the total array factor for the TAS (integral under the curve D) is $\approx$ 3 dB less than

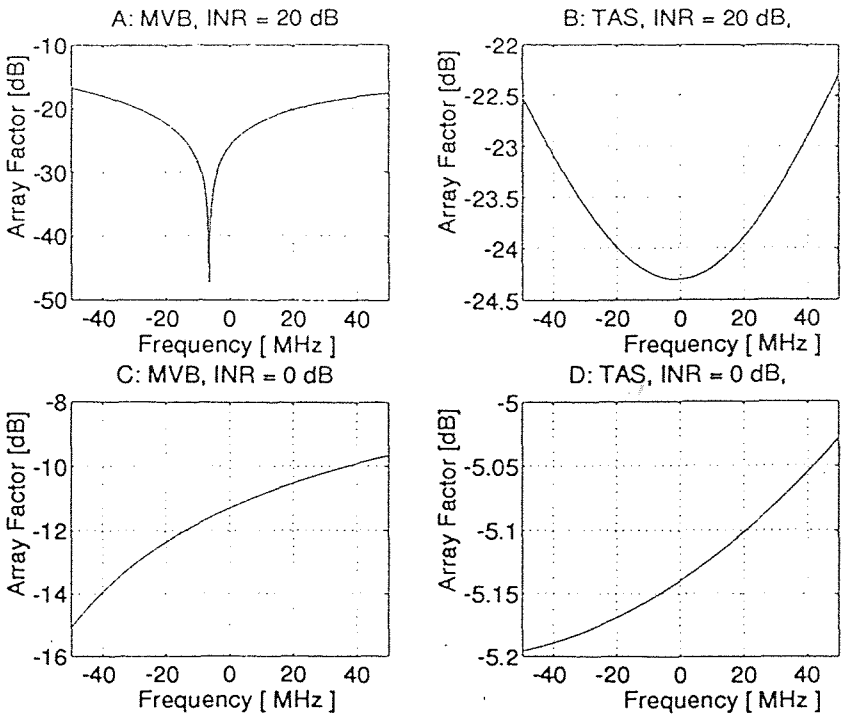

Figure 4.6 A comparison between MVB and TAS.

the total array factor for the MVB (integral under the curve C). This means that TAS would provide lower gain in the direction of the interference. It can also be observed from the sub-plot D that the gain of the TAS processor is limited within $\approx$ 2.5 dB interval (between -30.5 and -33 dB). The array factor of the MVB (sub-plot C) differs much more in the frequency interval under observation (from -25 dB at the edge of the band to -50 dB at the carrier frequency). It can be concluded that TAS becomes more effective comparing to the MVB as the bandwidth is increased.

Figure 4.6 illustrates how noise level at the input affects the MVB/TAS comparison. Plots are given for 10 % fractional bandwidth. Sub-plots A and B are calculated for the INR=20 dB. Calculating the total array factor (the integral under the curves) would give that TAS (sub-plot B) has $\approx$ 6 dB less total array factor in the direction of the interference than the MVB (sub-plot A). Results change if the

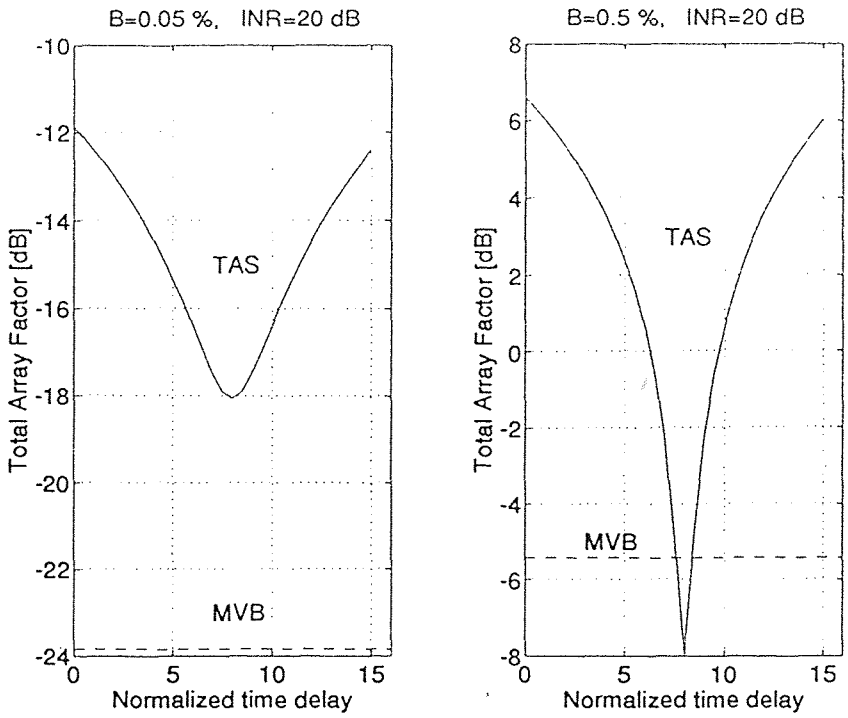

Figure 4.7 A comparison between MVB and TAS.

noise level is equal to the interference power at the input. This is shown on sub-plots C and D. Integrating the areas under the curves C and D would give $\approx$ 8 dB less total array factor for the MVB than for TAS. Higher noise level with respect to the interference (sub-plots C and D) at the input deteriorates the performance of both the MVB and the TAS processor. It affects TAS processor more than the MVB. While for INR=20 dB TAS provided 6 dB lower gain to the interference than the MVB, for INR=0 dB the MVB provided 8 dB lower gain than TAS. The conclusion is that TAS performs better with respect to MVB if the INR at the input is large enough.

Figure 4.7 shows the total array factor as a function of the normalized time delay. The total array factor is the integral of the array factor over all frequencies. The normalized time delay is t_d/τ_i, where t_d denotes the compensation time delay in

the auxiliary channel and τ_i is the propagation time delay across the array. Sub-plot A is drawn for 0.05 % fractional bandwidth (500 KHz around 1 GHz carrier) and sub-plot B is drawn for 0.5 % (5 MHz around 1 GHz). The 16-element array is observed. The minimum total array factor for TAS is obtained at $t_d = \frac{16}{2}\tau_i = 8\tau_i$, as given with (3.18). For B=0.05 %, the MVB (dashed line) performs better in the sense that it provides lower gain (total array factor) in the direction of the interference than the TAS processor. If the interference has a wider band, TAS achieves the lower total array factor when the optimal compensation time delay is implemented. This is shown on sub-plot B and the improvement is $\approx$ 3 dB. Wider frequency range of the interference signals degrades the performance of both the MVB and the TAS processor, but TAS is able to compensate some of the broadband effect by using frequency dependence due to the compensation time delay. So although the absolute performance of the TAS processor is worse if the bandwidth of the interference is larger, the performance relative to the MVB is improved. The conclusion from Figure 4.7 is that TAS has advantage over the MVB as the bandwidth of the interference is increased.

CHAPTER 5

OTHER CANCELLATION STRUCTURES

5.1 Introduction

While investigating the TAS method, ideas for other array structures emerged. In this chapter some of these ideas will be introduced. After the configuration of every structure is described, mathematical analysis will be presented. Derived expressions will be calculated for particular realizations. Three different array configurations are proposed. A time delay can be implemented in each of these configurations. Therefore, the structures are denoted as TAS2, TAS3, and TAS4. The unified analysis is done for each of them. The practical implementation is based on the estimation of the correlation matrices and cross-correlation vectors as proposed in the block diagram in Figure 3.4. There are some common assumptions used in each of the observed structures. The interference is assumed flat in the frequency region of interest. The power spectral density of the interference is taken to be one as opposed to the previous assumption when the interference power at the input was one. Additive noise is modelled as white Gaussian noise with zero mean and variance σ^2. The desired signal power is neglected as discussed in the Chapter 2. The direction of the desired signal is assumed known which enables using a vector of ones as the steering vector $\underline{d}_o$.

5.2 The TAS2 Structure

The TAS2 structure is sketched in Figure 5.1. The term TAS2 is somewhat misleading since TAS2 is in fact equivalent to the MVB. There is no benefit in using a compensation time delay for the configuration shown in Figure 5.1 and that will be shown later. Inputs to all sensors are added and normalized to give the gain of one in the direction of the desired signal at the output of the adder. The adder is denoted

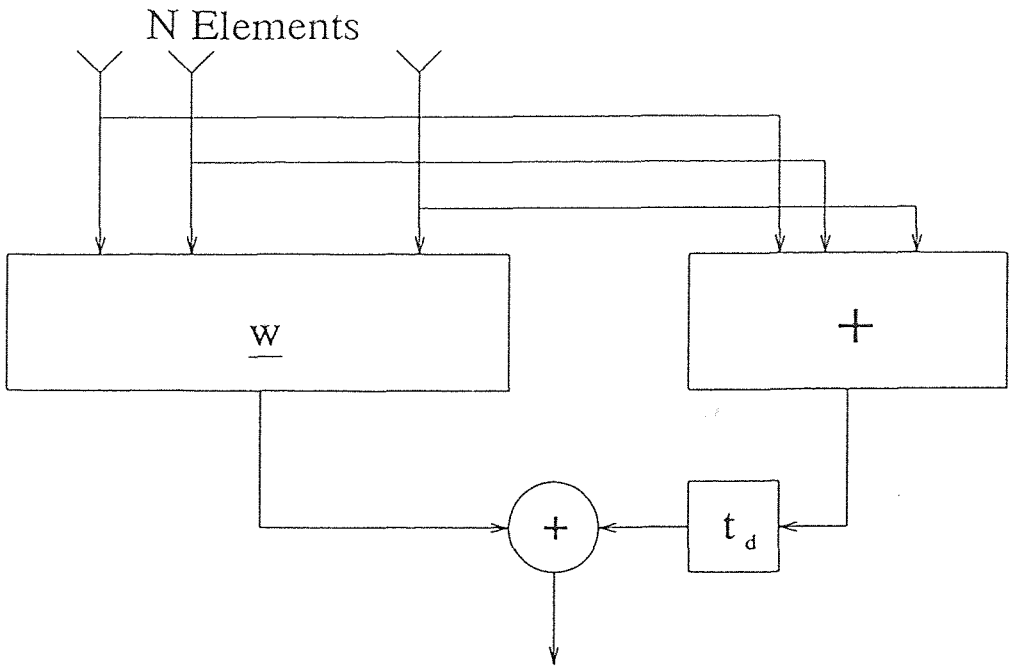

Figure 5.1 The TAS2 structure.

with + sign. Simultaneously, the inputs are adaptively weighted (denoted with w). The weighting is done under the constraint that the desired signal is cancelled at the output of the adaptive beamformer. Therefore, the desired signal is supplied from the adder with unitary gain due to normalization at the output of the adder. Time delay of the adder output is denoted with t_d, but it will be shown that no time delay can improve the performance of the TAS2 structure. The minimum output power is obtained for $t_d = 0$.

For the narrowband interference it can be proven that TAS2 gives the same residual power as the MVB. If the sum of the inputs are denoted as a, the objective is:

$$\text{Minimize } E[|a - \underline{w}^H \underline{x}|^2] \text{ subject to } \underline{w}^H \underline{d}_o = 0.$$

The residual power is:

$$p_{res} = E[|a - \underline{w}^H \underline{x}|^2] - \lambda(\underline{w}^H \underline{d}_o - 0). \tag{5.1}$$

Second term does not increase the residual power if the weight vector $\underline{w}$ satisfies the constraint $\underline{w}^H \underline{d}_o = 0$. The frequency does not appear in the equation above because the narrowband case is considered. Substituting:

$$\begin{aligned} p_\Sigma &= E[|a|^2] \\ \underline{u} &= E[a^* \underline{x}] \\ R &= E[\underline{x}\ \underline{x}^H], \end{aligned} \tag{5.2}$$

(5.1) develops into:

$$p_{res} = p_\Sigma - \underline{w}^H \underline{u} - \underline{u}^H \underline{w} + \underline{w}^H R \underline{w} - \lambda \underline{w}^H \underline{d}_o. \tag{5.3}$$

The optimal weight vector is obtained as:

$$\frac{\delta p_{res}}{\delta \underline{w}^H} = 0 \Rightarrow \underline{w}_{opt} = R^{-1}\underline{u} + \lambda R^{-1}\underline{d}_o. \tag{5.4}$$

Using the constraint $\underline{w}_o^H \underline{d}_o = 0$, the Lagrange coefficient becomes:

$$\lambda^* = -\frac{\underline{u}^H R^{-1} \underline{d}_o}{\underline{d}_o^H R^{-1} \underline{d}_o}. \tag{5.5}$$

The optimal weight vector is:

$$\underline{w}_{opt} = R^{-1}\underline{u} - \frac{(\underline{u}^H R^{-1} \underline{d}_o)^H}{\underline{d}_o^H R^{-1} \underline{d}_o} R^{-1} \underline{d}_o. \tag{5.6}$$

Substituting (5.5) and (5.6) into (5.3) and after few steps, the residual power becomes:

$$p_{res} = p_\Sigma - \underline{u}^H R^{-1} \underline{u} + |\lambda|^2 \underline{d}_o^H R^{-1} \underline{d}_o. \tag{5.7}$$

The advantage will be taken of the signal representation outlined in the Section 2.2. All assumptions made there, will be used here as well. The first term of (5.7) is the power of the adder output:

$$p_\Sigma = \frac{1}{N^2} E[|\sum_{k=1}^{N} d_{jk} + \sum_{k=1}^{N} n_k|^2], \tag{5.8}$$

where d_{jk} denotes the k-th component of the interference steering vector and n_k denotes the noise signal at k-th sensor. Factor $1/N^2$ is taken to normalize the gain for the desired signal at the output of the adder. After few steps, (5.8) becomes:

$$p_\Sigma = \frac{|s|^2}{N^2} + \frac{\sigma^2}{N}, \tag{5.9}$$

where s is defined as:

$$s = \sum_{k=1}^{N} d_{jk} = \sum_{k=1}^{N} e^{-j\omega_c \tau_i k} = e^{-j\omega_c (N+1)\tau_i/2} \frac{\sin(N\omega_c \tau_i/2)}{\sin(\omega_c \tau_i/2)}. \tag{5.10}$$

The cross-correlation vector $\underline{u}$ that appears in the middle terms is:

$$\underline{u} = E[a^* \underline{x}] = E[\frac{1}{N}(\sum_{k=1}^{N} d_{jk}^* + \sum_{k=1}^{N} n_k^*)(\underline{d}_i + \underline{n})], \tag{5.11}$$

where $\underline{n}$ denotes the vector of the noise components. After few steps (5.11) becomes:

$$\underline{u} = \frac{1}{N}(s^* \underline{d}_i + \sigma^2 \underline{d}_o). \tag{5.12}$$

The correlation matrix in the narrowband case is $R = \underline{d}_i \ \underline{d}_i^H + \sigma^2 I$ which completes definitions of the terms in (5.7).

Since everything is observed at the carrier frequency, the correlation matrix can be analytically inverted using the matrix inversion lemma ([12]):

$$R^{-1} = \frac{1}{\sigma^2}(I - \frac{\underline{d}_i \ \underline{d}_i^H}{\sigma^2 + N}). \tag{5.13}$$

In obtaining (5.13), $\underline{d}_i^H \underline{d}_i = N$ was used. Using (5.12) and (5.13),

$$\underline{u}^H R^{-1} \underline{u} = \frac{|s|^2 + \sigma^2 N}{N}. \tag{5.14}$$

Subtracting (5.14) from (5.9), zero is obtained which leaves only the third term in the expression for the residual power (5.7):

$$p_{res} = |\lambda|^2 \underline{d}_o^H R^{-1} \underline{d}_o. \tag{5.15}$$

Substitution of (5.5) for λ is made to obtain:

$$p_{res} = \frac{|\underline{u}^H R^{-1} \underline{d}_o|^2}{(\underline{d}_o^H R^{-1} \underline{d}_o)^2} \underline{d}_o^H R^{-1} \underline{d}_o. \tag{5.16}$$

After several steps,

$$\underline{u}^H R^{-1} \underline{d}_o = \frac{1}{N\sigma^2}(s\underline{d}_i^H + \sigma^2 \underline{d}_o^H)(I - \frac{\underline{d}_i \ \underline{d}_i^H}{\sigma^2 + N})\underline{d}_o = 1. \tag{5.17}$$

The final expression for the residual power is:

$$p_{res} = \frac{1}{\underline{d}_o^H R^{-1} \underline{d}_o}. \tag{5.18}$$

This is exactly the same as (2.21) and therefore it is proven that TAS2 is equivalent to the MVB in the narrowband case.

In the case of a wideband interference, the optimization problem is:

$$\text{Minimize } \int_{-\Delta\omega/2}^{\Delta\omega/2} |a(\omega)e^{-j\omega t_d} - \underline{w}^H \underline{x}(\omega)|^2 d\omega \text{ subject to } \underline{w}^H \underline{d}_o = 0.$$

This will lead to the same form as (5.3), but the terms are different due to the frequency dependence. These terms are:

$$p_\Sigma = \int_{-\Delta\omega/2}^{\Delta\omega/2} E[|a(\omega)|^2] d\omega = \int_{-\Delta\omega/2}^{\Delta\omega/2} (\frac{1}{N^2}|s(\omega)|^2 + \frac{\sigma_d^2}{N}) d\omega, \tag{5.19}$$

where $s(\omega)$ is defined as:

$$s(\omega) = \sum_{k=1}^{N} e^{-j(\omega+\omega_c)\tau_i k} = e^{-j(\omega+\omega_c)(N+1)\tau_i/2} \frac{\sin(\tau_i(\omega+\omega_c)N/2)}{\sin(\tau_i(\omega+\omega_c)/2)}. \tag{5.20}$$

Symbol ω denotes the baseband angular frequency. Instead of assuming that the total power of the interference is one, the power density is assumed one ($p_i/\Delta\omega = 1$). Therefore, $\sigma_d^2 = \sigma^2/\Delta\omega$ is the power density of the noise. The cross-correlation vector $\underline{u}$ is given as:

$$\underline{u} = \int_{-\Delta\omega/2}^{\Delta\omega/2} \frac{e^{j\omega t_d}}{N} E[(s^*(\omega) + \sum_{k=1}^{N} n_k^*(\omega))(\underline{d}_i(\omega) + \underline{n}(\omega))] d\omega. \tag{5.21}$$

Evaluating the expectation inside the integral, $\underline{u}$ becomes:

$$\underline{u} = \int_{-\Delta\omega/2}^{\Delta\omega/2} \frac{e^{j\omega t_d}}{N} (s^*(\omega)\underline{d}_i(\omega) + \sigma_d^2 \underline{d}_o) d\omega. \tag{5.22}$$

The correlation matrix appearing in the fourth term of (5.3) is the wideband correlation matrix derived in the Section 4.2.

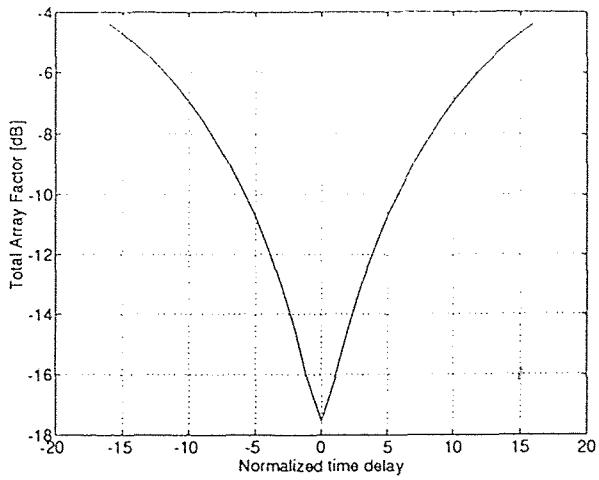

Figure 5.2 The effect of the time delay on the TAS2 structure.

Further analytic work is difficult since the integrals are analytically unsolvable. Therefore, the numerical methods must be used. The procedure is to calculate R_w (which can be done analytically for the flat interference spectrum as described in the Section 4.2). Then numerical integration must be used to calculate (5.22). The optimal weight vector can be calculated afterwards as given with (5.6). The first term of (5.3) must also be numerically calculated. This somewhat tedious procedure gives results that are identical to the wideband MVB. The Simpson formula ([2]) was used to calculate results for TAS2 and to check that both structures produce the same cancellation. This fact has been checked for different array parameters and no difference between the MVB and TAS2 was noticed.

It can be also shown that the time delay can not improve the performance of TAS2. This time delay is denoted with t_d in Figure 5.1. This is illustrated in Figure 5.2. The total array factor is plotted as a function of the normalized time delay. It can be observed that $t_d = 0$ (no time delay) gives the best results (the least total array factor in the direction of the interference). All elements create the output of the adder. There is no propagation delay between the beamformer output and the

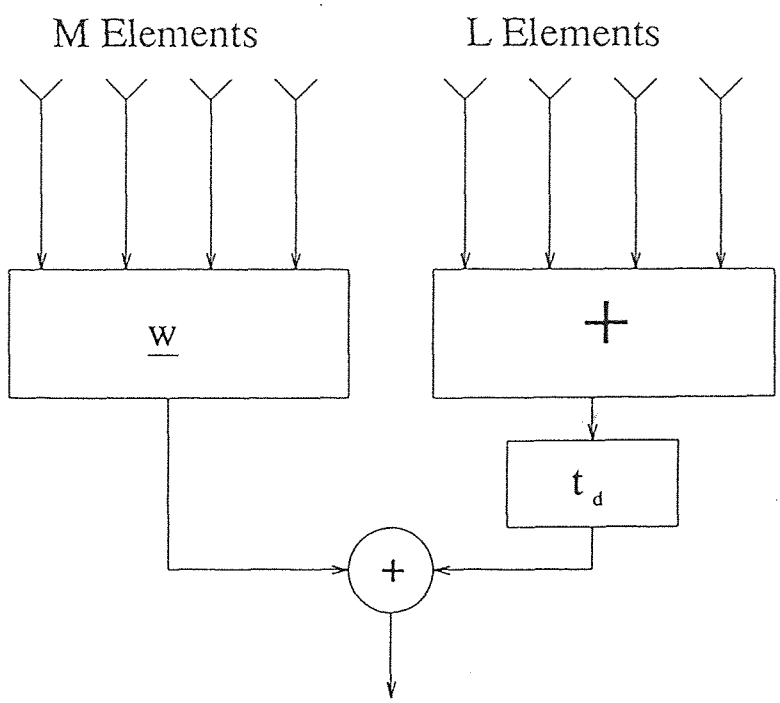

Figure 5.3 The TAS3 structure.

adder output to be compensated. Therefore, it can not be expected that a time delay could improve the cancellation after the subtraction from the beamformer.

5.3 The TAS3 Structure

The next array configuration to be examined is shown in Figure 5.3. The N-element array is partitioned into two subarrays. The outputs from the elements of the first subarray are added. The output of the second subarray is produced by the adaptive weighting of the subarray inputs. The weighting is done to minimize the residual power. The residual power is the power that is left after subtracting the subarray outputs. Before this subtraction, the adder output is time delayed. A mathematical analysis of the structure assumes that the first element of the L-element subarray is the reference. Therefore, M elements of the first subarray will have a positive propagation time delay $k\tau_i$, where k is the position of the sensor. Elements of the

second subarray on the right of the reference will have a negative propagation delay $-k\tau_i$.

The objective is:

$$\text{Minimize } \int_{-\Delta\omega/2}^{\Delta\omega/2} |a(\omega)e^{-j\omega t_d} - \underline{v}_M^H \underline{x}(\omega)|^2 d\omega \text{ subject to } \underline{v}_M^H \underline{d}_o = 0.$$

Subscript M denotes that the adaptive beamformer consists of M elements and $a(\omega)$ denotes the adder output. The residual power can be written in the same form as (5.3) which is repeated here for convenience:

$$p_{res} = p_\Sigma - \underline{v}_M^H \underline{u} - \underline{u}^H \underline{v}_M + \underline{v}_M^H R_w \underline{v}_M. \tag{5.23}$$

The solution for the optimal weight vector is given with (5.6). Developing (5.23), it can be shown that for the TAS3 structure, the cross-correlation vector is given as:

$$\begin{aligned} \underline{u} &= \int_{-\Delta\omega/2}^{\Delta\omega/2} \frac{e^{j\omega t_d}}{L} E[(s_L(\omega) + \sum_{k=1}^{L} n_k^-)(\underline{d}_i(\omega) + \underline{n}(\omega))] d\omega \\ &= \int_{-\Delta\omega/2}^{\Delta\omega/2} \frac{e^{j\omega t_d}}{L} s_L(\omega) \underline{d}_i(\omega) d\omega. \end{aligned} \tag{5.24}$$

Factor 1/L serves to normalize the adder output and subscript L denotes that $s_L(\omega)$ is the sum of L components of the interference steering vector:

$$s_L(\omega) = \sum_{k=0}^{L-1} e^{j(\omega+\omega_c)\tau_i k}. \tag{5.25}$$

Steering vector $\underline{d}_i$ has M components. There are no noise terms in the cross-correlation vector because different sensors are being correlated in the TAS3 array and the noise at different sensors is uncorrelated. The adder output power is given as:

$$\begin{aligned} p_\Sigma &= \int_{-\Delta\omega/2}^{\Delta\omega/2} E[|a(\omega)|^2] d\omega \\ &= \int_{-\Delta\omega/2}^{\Delta\omega/2} (\frac{1}{L^2} |s_L(\omega)|^2 + \frac{\sigma_d^2}{L}) d\omega. \end{aligned} \tag{5.26}$$

The correlation matrix R_w that appears in the fourth term of (5.23) is M-by-M. It correlates the input signals of the M-element beamformer. The components of R_w are given in (4.11).

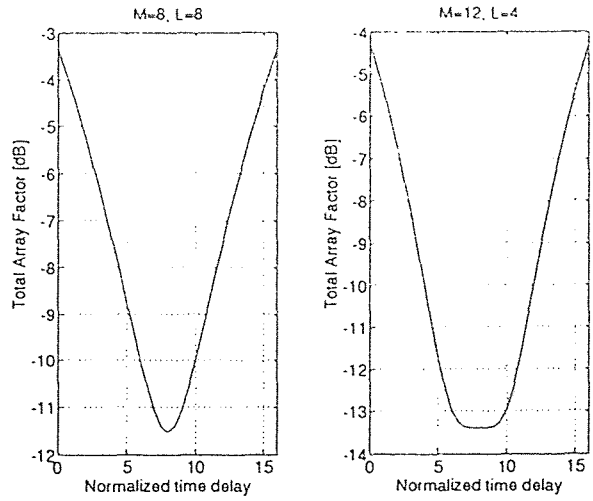

Figure 5.4 The effect of the time delay on two different TAS3 structures.

The interference array factor can now be calculated. The optimal subarray weight vector is given with (5.6) using proper R_w, $\underline{u}$, and $\underline{d}_o$ as applicable for the TAS3. The array factor to the interference is:

$$A_{iTAS3}(\omega) = |s_L(\omega)e^{-j\omega t_d} - \underline{v}_M^H \underline{d}_i(\omega)|. \tag{5.27}$$

Formula (5.27) is numerically calculated for two different partitions. The result is expressed in Figure (5.4). The initial 16-element array is partitioned into two subarrays. Sub-plot A shows how the total array factor depends on the normalized time delay for the partition M=8, L=8. Sub-plot B presents the partition L=4, M=12. It can be seen that the second partition performs better in terms of the array factor. There is obviously a number of combinations for a given number of array elements. Therefore, each array configuration has to be treated separately.

From the Figure 5.4 it is clear that the compensation time delay does help in the interference cancellation. While the TAS2 structure was equivalent as the MVB, the TAS3 structure is closely related to regular TAS introduced in the Chapter 3. Regular TAS is in fact a special case of TAS3 with L=1.

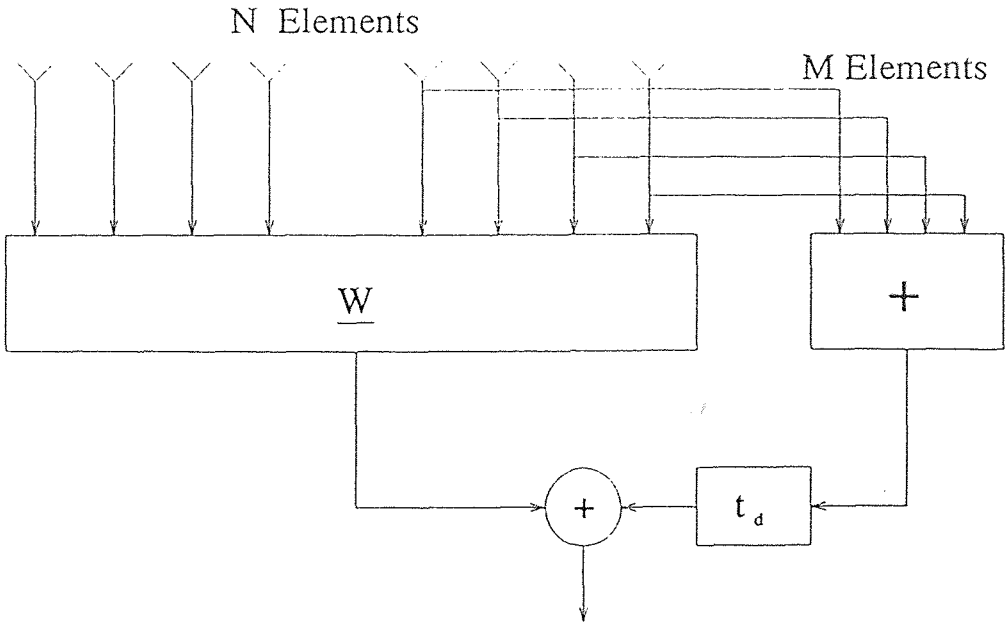

Figure 5.5 The TAS4 structure.

This section serves primarily to derive the mathematical basis and outline the procedure for calculating a general TAS case. The main idea from the Chapter 3 is extended for the auxiliary channel that is a sum of several sensors. The benefit is in the better noise averaging, because the new auxiliary channel will average noise on L elements. If only one element is used for the auxiliary channel, noise is passed unattenuated.

5.4 The TAS4 Structure

The TAS2 structure was shown to be equivalent to the MVB. It is not justified to implement a time delay since it makes the cancellation worse. This was illustrated in Figure 5.2. The TAS3 structure is similar to the regular TAS processor which was described in details in the Chapter 3. TAS3 is a more general case where elements can be combined in a number of ways. The TAS4 structure is a combination of TAS2 and TAS3. The configuration of TAS4 is shown in Figure 5.5. Inputs from the M

elements out of the N-element array are added (symbol +). In the same time, all inputs are adaptively weighted. This weighting is done as to obtain the minimum residual power. The residual power is the power that is left after subtracting the adaptively beamformed signal from the adder output. Since only M out of N elements are added, it can be expected that a time delay could help to compensate for the propagation delay. The compensation time delay is denoted with t_d. All previously accepted assumptions are used for the analysis of the TAS4 structure. The desired signal is cancelled in the adaptive beamformer and the output of the adder must be normalized to give the gain of one in the direction of the desired signal. This direction is assumed known. Similar analysis can be done as for the two previous structures. The procedure results in the familiar form for the residual power:

$$p_{res} = p_\Sigma - \underline{w}^H \underline{u} - \underline{u}^H \underline{w} + \underline{w}^H R_w \underline{w}. \tag{5.28}$$

For TAS4, the terms are defined as follows:

$$p_\Sigma = \int_{-\Delta\omega/2}^{\Delta\omega/2} E[|a(\omega)|^2] d\omega = \frac{1}{M^2} \int_{-\Delta\omega/2}^{\Delta\omega/2} (|s_M(\omega)|^2 + M\sigma_d^2) d\omega, \tag{5.29}$$

where $1/M^2$ normalizes the M-element adder output. The sum of the interference components in the adder will give:

$$s_M(\omega) = \sum_{k=1}^{M} e^{-j(\omega+\omega_c)k\tau_i} = e^{-j(\omega+\omega_c)\tau_i(M+1)/2} \frac{\sin(\tau_i(\omega+\omega_c)M/2)}{\sin(\tau_i(\omega+\omega_c)/2)}. \tag{5.30}$$

The cross-correlation weight vector is :

$$\underline{u} = \int_{-\Delta\omega/2}^{\Delta\omega/2} \frac{e^{j\omega t_d}}{M} E[(s_M^*(\omega) + \sum_{k=1}^{M} n_k^*(\omega))(\underline{d_i}(\omega) + \underline{n}(\omega))] d\omega, \tag{5.31}$$

where n_k denotes noise components at the M sensors whose outputs are added. The vector $\underline{n}(\omega)$ is N-by-1 vector of noise components at all N sensors. Autocorrelation of these terms will give vector $\underline{d_k}$ of the form:

$$\underline{d_k}^T = [\underbrace{\sigma_d^2 \quad \sigma_d^2 ..... \sigma_d^2}_{M} \quad \underbrace{0 \quad 0 ..... 0}_{N-M}]. \tag{5.32}$$

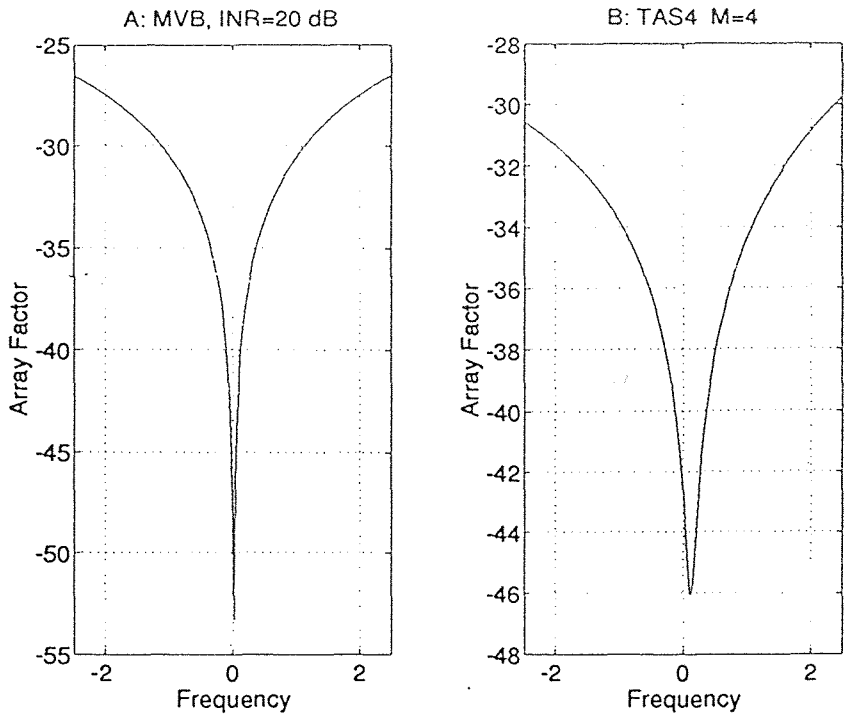

Figure 5.6 A TAS4 / MVB comparison.

The cross-correlation vector is:

$$\underline{u} = \int_{-\Delta\omega/2}^{\Delta\omega/2} \frac{e^{j\omega t_d}}{M} (s_M^*(\omega)\underline{d}_i(\omega) + \underline{d}_k)d\omega. \tag{5.33}$$

The components of the matrix R_w are given by (4.11).

The optimal weight vector is given with (5.6) and can be calculated using the proper R_w, $\underline{u}$, and $\underline{d}_o$. The interference array factor is:

$$A_{iTAS4}(\omega) = |s_M(\omega)e^{-j\omega t_d} - \underline{w}^H \underline{x}|. \tag{5.34}$$

In calculating the array factor (5.34), the Simpson formula ([2]) is used to evaluate integral (5.33). The numerical calculation is done for a 16-element array and 0.5 % fractional bandwidth relative to the carrier. The results are shown in Figure 5.6. Sub-plot A shows the array factor as a function of frequency for the MVB. If M=16 is taken (all sensors added, Figure 5.5), TAS4 becomes TAS2 and time delay does

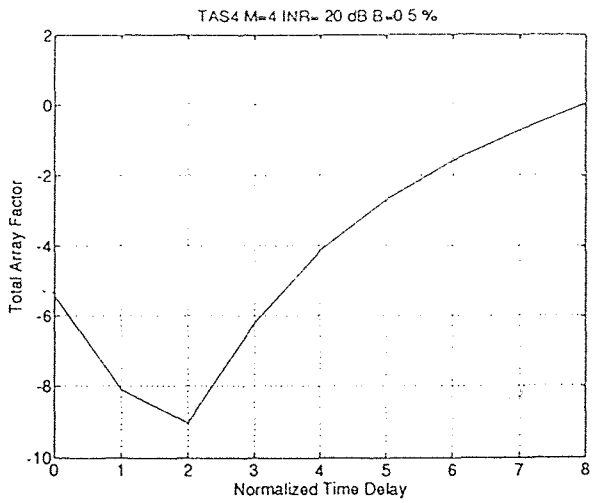

Figure 5.7 The optimal time delay for TAS4.

not help. Sub-plot B shows the result when 4 out of 16 elements are taken (M=4 at Figure 5.5). Since now not all elements are added in the adder, it can be expected that a compensation time delay could improve the array factor. The time delay produces a frequency dependent phase shift of the adder output. As illustrated on the sub-plot B, the improvement over the MVB is achieved even when arbitrary compensation time delay of $t_d = \tau_i$ is implemented. Numerical integration of the array factor over all frequencies gives ≈ -5 dB total array factor for the MVB (A) and ≈ -8 dB for TAS4 (B).

For the same configuration (M=4), the optimal time delay can be found. The total array factor is calculated as a function of the normalized time delay. The minimum of the total array factor determines the optimal compensation time delay. It can be observed from the Figure 5.7 that the optimal time delay is $t_d/\tau_i = 2$ (for the given set of array parameters). This time delay gives ≈ -4 dB less total array factor than the MVB (MVB gives $\approx$ -5 dB, and TAS4 with the optimal t_d gives $\approx$ -9 dB). Figure 5.7 is plotted for the resolution in time delay of $\tau_i/2$.

Figures 5.6 and 5.7 show only one particular realization of the TAS4 structure. Many other scenarios were investigated for each structure (MVB, TAS, TAS2, TAS3, and TAS4). It can be concluded after this investigation that TAS4 is the best structure in terms of the interference array factor. It means it would produce the least total gain in the frequency region of interest. Therefore, the TAS4 will attenuate a directional interference the most comparing to other investigated structures.

CHAPTER 6

COMPUTER SIMULATION

Numerical results presented so far were obtained by calculating the formulas. These formulas describe the idealized mathematical model. The assumptions were used in creating this model. Additive thermal noise was assumed to be Gaussian with zero mean and given variance. A directional interference was taken with a flat spectrum. In the wideband case, integrals were calculated numerically using the Simpson formula. The power of the desired signal was neglected. Adding a desired signal would not change results as shown in [15].

Calculated results were tested with a computer simulation. The simulation was modelled as follows (Figure 6.1):

A random sequence of samples is created to represent the received signal in the time domain. Discrete Fourier transform (DFT) gives the frequency counterpart of the time sequence. The frequency domain input vector is used to form a correlation matrix. This correlation matrix is calculated as an average of the outer product of the input signals:

$$\tilde{R} = \frac{1}{L} \sum_{l=1}^{L} \underline{x}_l \ \underline{x}_l^H, \tag{6.1}$$

where $\underline{x}_l$ is the l-th snapshot of the input vector and L is the number of snapshots taken. The speed and the quality of the real-time estimation depends on the value of L. There is a trade-off between these two properties. If L is large it would mean better estimation, but slower than in the case of fewer snapshots. It was found during the simulation that even only few snapshots $\underline{x}_l \ \underline{x}_l^H$ give results that are close to idealized results that were obtained calculating the formulas. The angle of arrival of the desired signal is assumed known. That allows us to work with the desired signal as if it comes from the boresight direction. This can be adjusted by simple phase

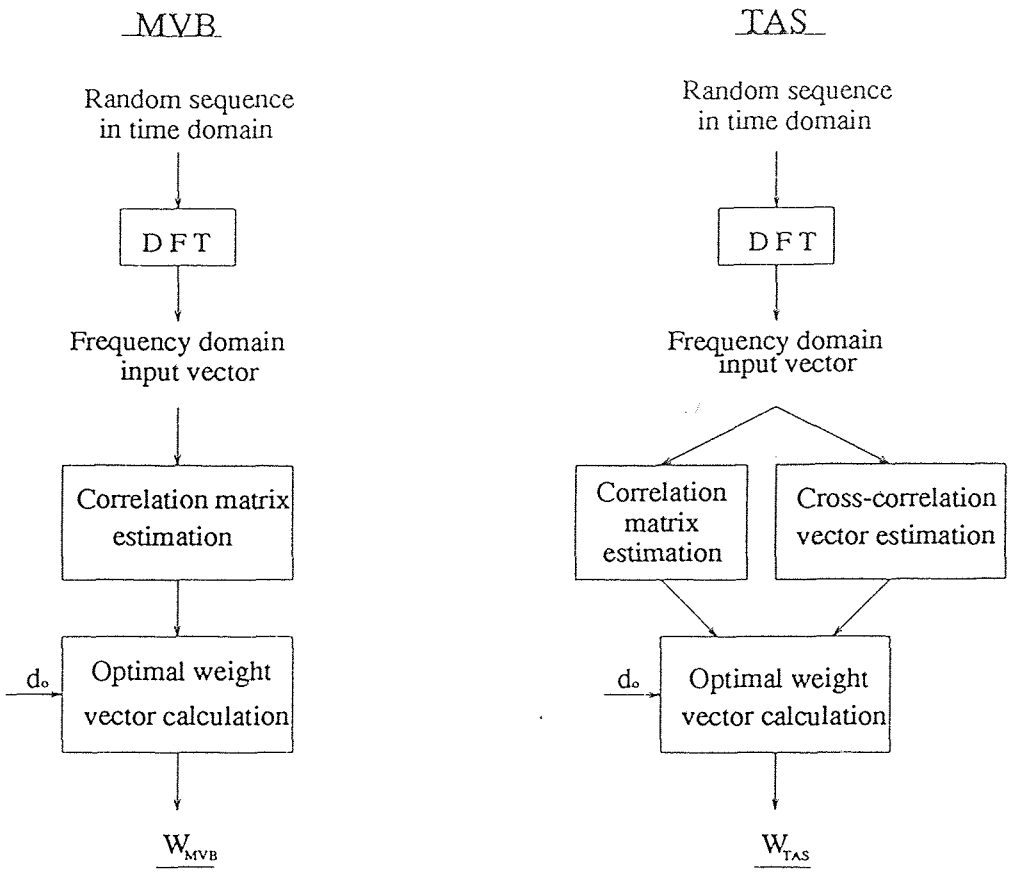

Figure 6.1 Simulation model flow-chart.

shift in every sensor. Under this assumption, the steering vector in the direction of the desired signal is vector of ones.

Now MVB solution can be found as explained in the Chapter 2:

$$\underline{w}_{MVB} = \frac{\tilde{R}^{-1}\underline{d}_o}{\underline{d}_o^H \tilde{R}^{-1}\underline{d}_o}. \tag{6.2}$$

For the TAS processor the cross-correlation vector must be estimated in addition to the correlation matrix. The direct estimation gives:

$$\underline{\tilde{u}}(\omega) = \frac{e^{j\omega t_d}}{L}\sum_{l=1}^{L} X_{ol}^{*}(\omega)\underline{x}_l(\omega), \tag{6.3}$$

where L denotes the number of snapshots, X_{ol} is the l-th snapshot of the auxiliary channel output, $\underline{x}_l$ is the l-th snapshot of the subarray input vector, and $*$ denotes

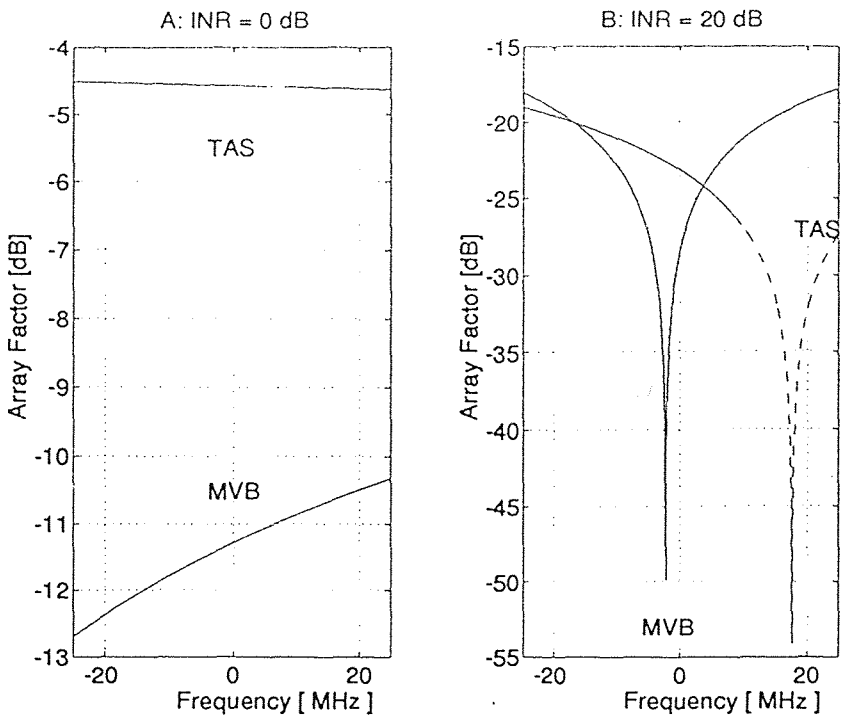

Figure 6.2 The effect of the noise level on the cancellation

the complex-conjugate operator. The TAS solution for the optimal subarray weight vector is:

$$\underline{v}_o = \tilde{R}^{-1}\underline{\tilde{u}} - \frac{(\underline{\hat{u}}^H \tilde{R}^{-1}\underline{d}_o)^*}{\underline{d}_o^H \tilde{R}^{-1}\underline{d}_o}\tilde{R}^{-1}\underline{d}_o. \tag{6.4}$$

With the weight vectors known, the array factors are:

$$A_{iMVB} = |\underline{w}_{MVB}^H \underline{d}_{i(N+1)}(\omega)| \tag{6.5}$$

$$A_{iTAS} = |e^{j\omega t_d} - \underline{w}_{TAS}^H \underline{d}_{iN}(\omega)|. \tag{6.6}$$

The subscripts N and N+1 by the steering vectors denote their dimension. The expressions (6.5) and (6.6) were derived in more details in the previous chapters.

The simulation model is presented in a form of a flow-chart that is sketched on the Figure 6.1. The only difference between the MVB and TAS is the cross-correlation vector needed in TAS. The array response is determined once the weight vector is calculated (expressions (6.5) and (6.6)). The array factor obtained using the

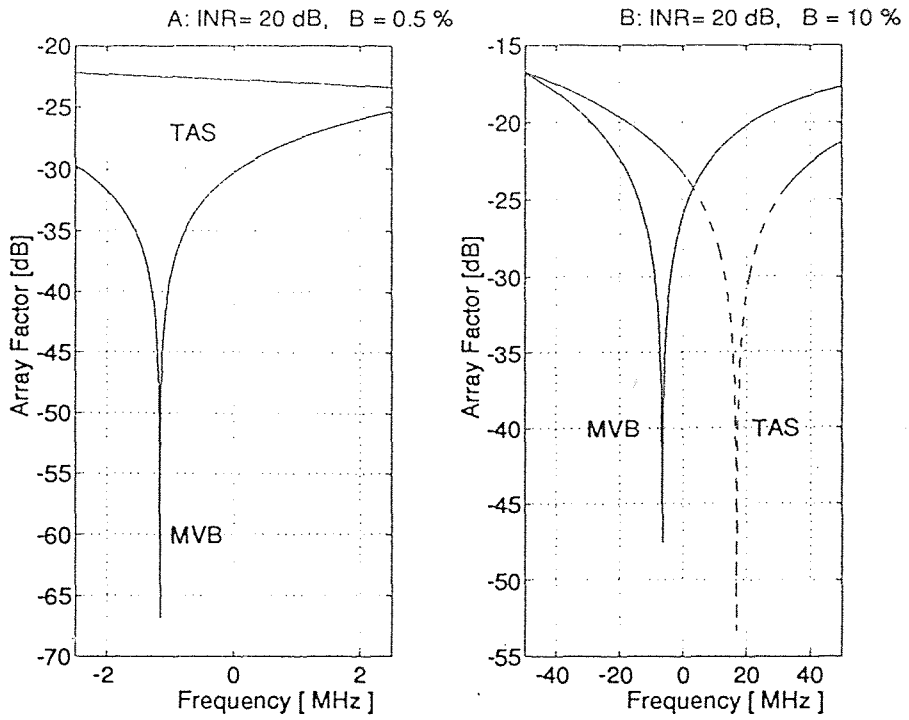

Figure 6.3 The effect of the bandwidth on the cancellation

outlined procedure is calculated for several array configurations. The array factor determines the gain that the array would provide in the direction of the steering vector. Plotted as a function of frequency, the array factor shows a frequency response in a specific direction. Figure 6.2 compares the array factors for the MVB and the TAS case. Sub-plot A shows that the MVB provides better cancellation when INR=0 dB (the same power of the interference and noise at the input). Sub-plot B shows the case when INR=20 dB. Both array factors are improved, but this improvement is more significant for TAS which achieves better cancellation than the MVB. This is consistent with the result from the idealized formula calculation. It shows that lower noise power level at the input (or the increase in the interference power) improves the TAS cancellation and can make it better than the MVB.

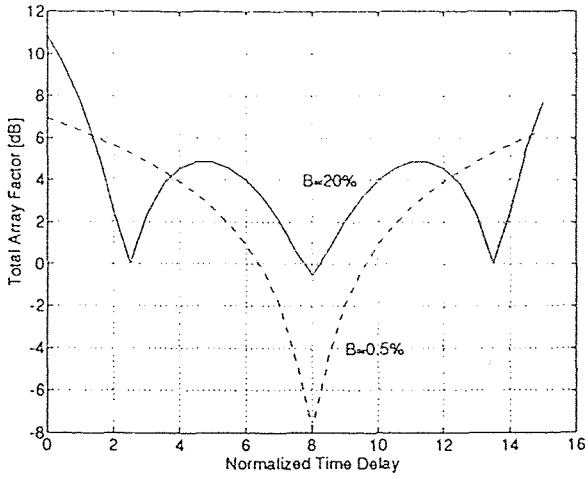

Figure 6.4 The optimal time delay

Figure 6.3 shows the effect of the bandwidth on the MVB/TAS comparison. Sub-plot A is given for 0.5 % fractional bandwidth. Sub-plot B is given for 10 % fractional bandwidth. It can be noticed that the MVB has advantages when the interference occupies narrower frequency band. When the bandwidth is increased, TAS improves compared to the MVB. This improvement is only relative because both the MVB and TAS perform worse if the bandwidth is increased. However, TAS can compensate a part of the broader band effects. The compensation is due to the frequency dependent weight vector (time delay implementation). This behaviour was also predicted with the calculation in the Chapter 4.

Figure 6.4 shows the optimal time delay for the 16-element array. For the narrowband case, B=0.5 % (dashed line), there is only one minimum corresponding to $t_d = (N+1)\tau_i/2$, where (N+1) is the total number of elements (+1 denotes the auxiliary channel). This was proven in section 3.4. For the wideband case, B=20 %, multiple minima occurred. This behaviour is attributed to the periodicity of the trigonometric functions. The strict mathematical treatment is not available. The reason is that the wideband correlation matrix is not analytically invertible. Multiple

minima were obtained also in the calculations in the Chapter 4. Thus, the simulation presented on the flow-chart 6.1 gives results which are consistent to the calculations based on the idealized model.

CHAPTER 7

CONCLUSION

This thesis investigated a new method for the interference cancellation. The special emphasis was given to the problem of nulling the wideband directional interference. The method is based on the adjustment of the sampling time in one or more of the array elements. Time adjustable sampling introduced a frequency dependence in the auxiliary channel. This frequency dependence is in addition to the adaptive beamforming in the subarray.

The method is in fact the linear prediction applied to antenna arrays. The subarray output needs to predict the output from the auxiliary channel with the least squared error. This will provide the best cancellation when the signal from the auxiliary channel is subtracted from the subarray output. The signal processing problem is to find the optimal weight vector. The components of the optimal weight vector are coefficients which are used in the subarray to achieve the prediction.

It was shown that the proper time delay in the auxiliary channel improves the wideband linear prediction significantly. The optimal time delay depends on the number of elements and the propagation time delay. For the narrowband interference source, it was possible to derive the optimal time delay. Using this delay in the auxiliary channel, the lowest residual power was obtained. In the wideband case there are more than one time delay that provide the minimum residual power. The effect of the bandwidth and the noise level was examined. The increase in both the noise level and the bandwidth made the cancellation worse.

The cancellation using linear prediction (TAS) was compared to a conventional adaptive array processing (MVB). The comparison was made in terms of the array factor, i.e. the gain in the certain direction. It was found that the optimal time delay can make TAS to have a lower array factor than the MVB. However, the MVB

is able to achieve better SNIR than the TAS processor. The reason is averaging the noise across the array in the MVB while the auxiliary channel in TAS passes the noise without attenuation. Both methods achieve the cancellation of directional interference compared to thermal noise. Therefore, the benefits of the lower array factor for the TAS processing are not a great advantage over the MVB in the noisy environment. The residual interference will be covered in the noise in the output signal.

Often the additional methods are used in radar to improve signal-to-noise ratio at the output of the receiver. The reason for this is the fact that radar deals with signals that contain weak desired signals compared to noise. Usually the special processing methods are needed to recover directional signals which are embedded in thermal noise (thermal noise is not directional in character). It was shown that TAS can cancel directional interference better than the MVB. If signal-to-noise ratio is increased at the output of the receiver, the benefits of the better cancellation of directional interference become more important.

The advantage of TAS over the MVB is also in the simpler implementation. The algorithms for the linear prediction ([11]) are computationally less involved and are more suitable for a real-time implementation.

Several additional issues were addressed in the thesis. The modular TAS was introduced. Several other structures were also introduced. They were denoted as TAS2, TAS3, and TAS4. The equivalence of the MVB and TAS2 was shown. TAS3 is the general case of TAS where the subarray predicts the sum of signals instead of a single signal. TAS4 provided the lowest array factor if implemented with a proper time delay. The mathematical model was created to treat each of these configurations. This model enables calculations for a given set of the array parameters. A computer simulation was performed and the calculation results are confirmed.

To reiterate, the applicability of the linear prediction for the wideband interference cancellation was the most important result out of the research. It was shown that time adjustable sampling improves the frequency response of linear arrays. The possible work to follow could include the investigation of the applicability of TAS for the sidelobe canceller. Configurations other than linear arrays (planar, circular) can also be treated with TAS. Combining the frequency focusing and TAS is expected to enable the treatment of the interference that is correlated with the desired signal. Simultaneous forward/backward linear prediction could provide further improvement. Forward/backward linear prediction amounts to using TAS in more than one channel.

REFERENCES

1. S. Applebaum, "Adaptive array," *IEEE Trans. Antennas and Propagation*, September 1976.

2. I. N. Bronstein, *Matematicki Prirucnik*, Skolska Knjiga, Zagreb, Croatia, 1983.

3. B. Carlson, "An ultralow sidelobe adaptive array antenna," *The Lincoln Laboratory Journal*, March 1990.

4. R. T. Compton, *Adaptive Antennas, Concepts and Performance*, Prentice-Hall, Engelwood Cliffs, New Jersey, 1988.

5. W. C. Cummings, A. J. Simmons, and T. J. Mayhan, "Wideband adaptive antenna nulling using tapped delay lines," *IEEE Trans. Antennas and Propagation*, November 1981.

6. O. L. Frost, "An algorithm for linearly constrained adaptive array processing," *Proc. IEEE*, August 1972.

7. W. F. Gabriel, "Adaptive arrays: An introduction," *Proc. IEEE*, February 1976.

8. A. L. Garcia, *Probability and Random Processes for Electrical Engineering*, Addison-Wesley, Reading, MA, 1989.

9. L. J. Griffiths, "A simple adaptive algorithm for real time processing in antenna arrays," *Proc. IEEE*, October 1969.

10. S. Haykin, *Communications Systems*, Wiley, New York, 1983.

11. S. Haykin, *Adaptive Filter Theory*, Prentice Hall, Engelwood Cliffs, New Jersey, 1991.

12. J. E. Hudson, *Adaptive Antenna Principles*, The Institution of Electrical Engineers, London, 1981.

13. C. W. Jim, "A comparison of two lms constrained optimal array structures," *Proc. IEEE*, December 1977.

14. J. T. Mayhan, "Some techniques for evaluating the bandwidth characteristics of adaptive nulling systems," *IEEE Trans. Antennas and Propagation*, May 1979.

15. T. W. Miller and R. A. Monzingo, *Introduction to Adaptive Arrays*, John Wiley and Sons, New York, 1980.

16. A. Papoulis, *Probability, Random Variables, and Stochastic Processes*, McGraw-Hill, Inc., New York, 1991.

17. S. Simanapalli and M. Kaveh, "Broadband focusing for partially adaptive beamforming," *IEEE Trans. Aerospace and Electronic Systems*, 1994.

18. G. Strang, *Linear Algebra and its Applications*, Harcourt, Brace, Jovanovich Publishers, San Diego, 1988.

19. G. Swisher, *Introduction to Linear System Analysis*, Matrix Publishers, Champaign, IL, 1976.

20. J. Teti et al., "Wideband airborne early warning radar," *Proc. IEEE*, April 1993.

21. D. W. Tufts and R. Kumaresan, "Estimation of frequencies of multiple sinusoids: Making linear prediction perform like maximum likelihood," *Proc. IEEE*, September 1982.

22. W. D. White, "Wideband interference cancellation in adaptive sidelobe cancellers," *IEEE Trans. Aerospace and Electronic Systems*, November 1983.

23. B. Widrow et al., "Adaptive antenna systems," *Proc. IEEE*, December 1967.

24. E. Zentner, *Radiokomunikacije*, Skolska Knjiga, Zagreb, Croatia, 1987.